THE UNSATURATED SHEAR STRENGTH AND SWELLING CHARACTERISTICS OF EXPANSIVE SOILS OF ARBA MINCH

A Thesis Submitted to
School of Graduate Studies of Addis Ababa University
In Partial Fulfillment of the Requirement for the Degree of
Master of Science in Civil Engineering

By

BANTAYEHU UBA

Advisor

HADUSH SEGED (PhD)

June 2011
Addis Ababa, Ethiopia.

ADDIS ABABA UNIVERSITY
SCHOOL OF GRADUATE STUDIES

THE UNSATURATED SHEAR STRENGTH AND SWELLING CHARACTERISTICS OF EXPANSIVE SOILS OF ARBA MINCH

By

BANTAYEHU UBA

June 2011

Approved by Board of Examiners

Dr. Hadush Seged__	_____	_____
Advisor	Signature	Date
Prof. Alemayehu Teferra__	_____	_____
External Examiner	Signature	Date
Dr. Samuel Taddese__	_____	_____
Internal Examiner	Signature	Date
Ato. Demelsha_Samuel__	_____	_____
Chair-man	Signature	Date

To: Etenesh Uba

Acknowledgements

Praise and thanks be to God almighty, the most gracious and the most merciful, for giving me the ability, the health, and the strength to finish this work.

I would like to express my deepest appreciation to my advisor, Dr. Hadush Seged for his endless encouragement, material supply, valuable and continuous guidance through the course of this study, and for the time in proofing the manuscript.

Special thank goes to Mr. Kahsay Hagos, Senior material inspector in Transport Construction Design Share Company (TCDE) on Arba Minch – Jinka Road project, and Mr. Haymanot Kebede, Project Engineer in Rama Construction on AMU health campus construction project, for their help in material, man power and transport arrangement during sample extraction.

I wish to express my gratitude to Mr. Tamirat Tafesse and Mr. Mihretu Tessema, for their encouraging mentoring that let me to stay persistent and curious. Special thanks are extended to Mr. Biruk Tesfaye, Mr. Bisrat Brihane, and all of my friends who motivated and assisted me in different phases of the study. Gratitude expressed to Mr. Getaneh W/Medhin for his continuous support and patience in sharing his experience of testing and operation with the modified triaxial machine, which could not be left unmentioned.

I wish also to appreciate the kindness and assistance of the entire Geotechnical engineering laboratory technicians during the experimental work.

Last, but in no sense the least, I would like to express my sincere thanks to my family for their constant encouragement, and moral support without which this study would not be done.

Table of Contents

List of Symbols

u_a	Pore air Pressure
u_w	Pore water Pressure
h_m	Matric suction
π	Osmotic suction
CU	Consolidated undrained
c'	Effective cohesion
$\varnothing'$	Effective internal angle of friction
$\varnothing^b$	Angle indicating the rate of increase in shear strength relative to matric suction
τ	Shear stress
σ	Normal stress
χ	Effective stress parameter
C	Clay size fraction finer than 0.002mm
ω	Moisture content
γ_d	Dry density
LL	Liquid limit
PI	Plasticity index
PL	Plasticity limit
SI	Shrinkage index
SL	Shrinkage limit
Sp	Swelling pressure
Ac	Activity
BS	British Standard Methods of test
ASTM	American Society for Testing and Materials
AASHTO	American Association of State Highway and Transportation Officials
USCS	Unified Soil Classification System
ROSA	Resource Oriented Sanitation concepts for peri-urban areas in Africa
CSA	Central Statistics Authority
AMU-HSC	Arba Minch University Health Science Collage

List of Tables

List of Figures

List of Tables in Appendixes

List of Figures in Appendixes

Abstract

In Ethiopia, so many researches were done on characterizing expansive soils of several towns but only a single study, done on Addis Ababa expansive soil, exists on the unsaturated shear strength behavior of expansive soils. The present study addresses examining the expansive soils in Arba Minch – a town with a great portion of its terrain covered by the same soil but not considered in previous studies. A laboratory-testing program was planned and carried out on undisturbed soil samples taken from 10 different locations in the town for swelling pressure testing; and among these, one pit was allotted for unsaturated shear strength study.

The laboratory test results revealed that the swelling pressure ranges from 74.53 to 571.29 kPa, Specific Gravity from 2.63 to 2.80, Plasticity Index from 49 to 77%, Shrinkage Index from 81 to 117% and Free Swell from 94.0 to 165.0%. The measured swelling pressures and the geotechnical parameters determined from identification tests are used to assess the validity of already developed expressions by various researchers to the site under study and new models, that relate swelling pressure with index and physical properties, are developed using SPSS16.0 for windows software.

The results from unsaturated shear strength tests performed with a 50kN modified double wall triaxial machine on an undisturbed sample setting matric suction to be 100 kPa, 150 kPa and 200kPa for an effective consolidation pressure of 200kPa have clearly indicated the saturated case to yield smaller shear strength than the unsaturated one. The maximum deviator stress showed to increase from 107.61kPa to 174.35kPa with an increase in matric suction but the shape of the stress-strain diagram remained identical.

1. INTRODUCTION

1.1. The Present Problems of Expansive Soils

The worldwide spread problematic expansive soil has got a great deal of attention so many years ago after its alarming amount of damage in the locality of its occurrence. Since then the areas of research focused on examining the nature and mechanism of swell-shrink behavior and developing empirical equations trying to predict the swelling pressure from the basic soil index properties. However, several considerations within the past two decades or so have shown an increasing interest of geotechnical investigators in the unsaturated state of these soils upon the development of advanced testing equipments and techniques, which permit the control of pore-air pressure in the test sample.

Expansive soils are clay soils with high plasticity (i.e. high liquid limit) known for their peculiar nature of expanding or shrinkage when exposed to moisture changes. During dry seasons, they shrink forming cracks and swell during wet periods causing most damage to structures particularly light buildings such as houses, apartments, warehouses, small industrial buildings, and pavements in several areas of the world. Aytekin (1992) explained that, in the United States alone, expansive clay have been estimated to produce annual damages of $1.7 billion on streets and highways and more than $9.0 billion on all structures on expansive soils. The damage turns to be more than double the cost associated with repair to damage from floods, hurricanes, tornadoes, and earthquakes (Al-Rawas and Goosen, 2006; Nelson and Miller, 1992; Chen, 1988). As well, in Sudan, expansive soils have caused an estimated annual damage of $6.0 million to irrigation systems, water lines, sewer lines, buildings, roads, and other structures (Charlie et al., in Aytekin, 1992).

The problems with expansive soils are still manifested globally. Ethiopia is among the countries that have reported internationally their problems at research conferences (Fredlund and Rahardjo, 1993). The damages will be much greater in coming years if expansive soils are not recognized before builders start to build structures in/on expansive soils (Aytekin 1992). Sisay (2004), under his study on damage assessment of buildings constructed on expansive soils of Addis Ababa, has found 64% of the randomly surveyed buildings to be adversely affected. Similarly, Sime (2006) indicated that most of the roads constructed failed before their expected design life, in some

cases after few months of completion and Teklu (2003) on his study on swelling pressure of Addis Ababa expansive soil also enlightened a lot of damages being occurring to civil engineering construction due to expansive soils, even if no organized economic survey has been made in the country. ROSA (2009) in their sanitation project in Arba Minch town indicated a significant portion of the town to comprise loose black cotton soil in which pit collapse is a major problem. Additional researches done on Addis Ababa, Mekelle, Bahir Dar, Gambela and Hawassa confirm that much has been done on characterizing the behaviour of the expansive soil and its distribution in Ethiopia (Gebrekristos, 2005; Legesse, 2004; Tilahun, 2007; Zewdie, 2004).

The degree of expansiveness depends on whether the soil mass contains active clay minerals or not. The three most important groups of clay minerals are Montmorillonite, Illite, and Kaolinite, which are crystalline hydrous aluminosilicate. Of these groups, Montmorillonite is the clay mineral that is mostly present in expansive soil and responsible for its expansive nature. When these minerals are exposed to moisture, water is absorbed between the inter-layering lattice structures and exerts an upward pressure, which is the cause for most damages associated with expansive soil. The damages can occur within a few months following construction, may develop slowly over a period of about 5 years, or may not appear for many years until some activity occurs to disturb the soil moisture (Chen, 1988; Teklu, 2003).

1.2. Motivation and Objective of the Study

A series of international conferences have been held to help cope with the expansive soil problem (Abed, 2008; Fredlund and Rahardjo, 1993). Worldwide, a significant amount of research has been carried out in the past to understand the swelling behaviour of these soils and the mechanisms involved therein. The outcomes of these investigations forwarded various forms of empirical equations which relate swelling behaviour to certain physical properties of the soil which are well understood by practicing engineers. The developed equations are easy to apply and give satisfactory results when applied to the particular soils for which they were developed.

As mentioned above, in Ethiopia, most research works on expansive soils were concentrated around Addis Ababa whilst very little have been made on regional town. The focus of the researches was somewhat inclined on its characterization, blending it with chemicals to mitigate

its poor quality, the damages it resulted and its distribution in Ethiopia but Tilahun (2004) in continuation to the work of Zewdie (2004) studied its shear strength characteristic based on Unconsolidated Undrained triaxial tests (UU) performed on saturated and unsaturated samples apprizing that suction can have major influence on the shear strength. Recently, Gebre (2010) has carried out the unsaturated shear strength characteristic and stress-strain behaviour of expansive soils still from Addis Ababa. However, depending upon the type of material, climate and topography, the engineering properties of expansive soils varies from place to place (Chen, 1988); thus requiring the behaviour of the same soil to be investigated in the other localities of the country. Arba Minch, which is located about 500 km south of Addis Ababa, is one of the towns where no such investigation has been conducted so far, even though expansive soil of residual deposit type covers most of its terrain.

In this thesis, the main objectives are:

1. to investigate the swell potential and swelling pressure of expansive soils of Arba Minch.
2. to study the unsaturated shear strength characteristic of the same soil.

1.3. Description of the study area

Arba Minch, with a population of 75,000 and annual population growth rate of 4.5% is one of the fast growing towns in Ethiopia. It was founded in 1960s and received its name from the abundant local springs which produce a groundwater forest. The town is located in Gamo Gofa zone, the Southern Nations, Nationalities and Peoples Region. To put this in a geographical positioning way, Arba Minch is located at the floor of the southern part of the East African Rift Valley between $6^0$30'N to $6^0$08'N latitude and $37^0$33'E to $37^0$37'E longitude at an elevation of 1285m above sea level (ROSA, 2009; Belachew, 2000; CSA, 2007).

Arba Minch town consists of the uptown administrative centre of Shecha and 4km away the downtown commercial and residential areas of Sikela, which are connected by a paved road. Recently, it is divided into four sub-cities which are restructured into eleven administrative kebeles. The area administered by the municipality extends up to 20.8km^2 and the expansion is fast particularly after 1980's due to the establishment of different institutions and rapid flow of rural migrants. The climate of Arba Minch area is categorized as semi-arid. The mean annual

rainfall, temperature, humidity, sunshine hours are about 750mm, 25^0C, 57%, 7.5 hours, respectively (ROSA, 2009; Belachew, 2000).

Geologically, the area belongs to the category of the Rift Valley system. The geological units in the Rift Valley region are mainly the result of volcanic activity during the Tertiary period. The whole Rift Valley is underlain by ancient basement rocks, which are defined as genesis grading in metamorphic granites, ignimbrites (consolidated hot-ash flows) and granodiorites. A more recent layer of volcanic rocks and ignimbrites has been added over the basement (Dagalo in Förch, 2009). Dagalo in Förch (2009) again referred basaltic flow and related spatter cones to be the major geologic units from which the well-known 'forty springs' flow. Resource Oriented Sanitation concepts for peri-urban areas in Africa – ROSA (2009) in their sanitation project of the town indicated a significant portion of the town to comprise loose black cotton soil in which pit collapse is a major problem. They highlighted the other part by saying to have rocky ground where digging is very difficult.

1.4. Scope of the Investigation

In order to address the aforementioned purposes, ten test pits were dug in the town at different locations where expansive soils prevail as part of this work. The sites for the test pits were selected systematically and are depicted in Figure 1.1. Undisturbed and disturbed samples were extracted from each test pit for Swelling pressure, Shear strength, and Index property tests. Among the rest, one pit was chosen for further unsaturated shear strength characteristic investigation where only undisturbed samples being used for both the conventional and the modified triaxial testing.

The depth of the pits varied from 1.0m to 2.5m (as it is frequent on the study area to place the foundation around these depths unless a basement construction forces further). The results from this research can be used in identifying and estimating the behaviour of the expansive soil of the area so that possible measures can be taken to reduce the problems arising to the structures during and after construction. It can also serve as a resource for further investigation on expansive clay soil, especially the unsaturated state, in the other locality of the country.

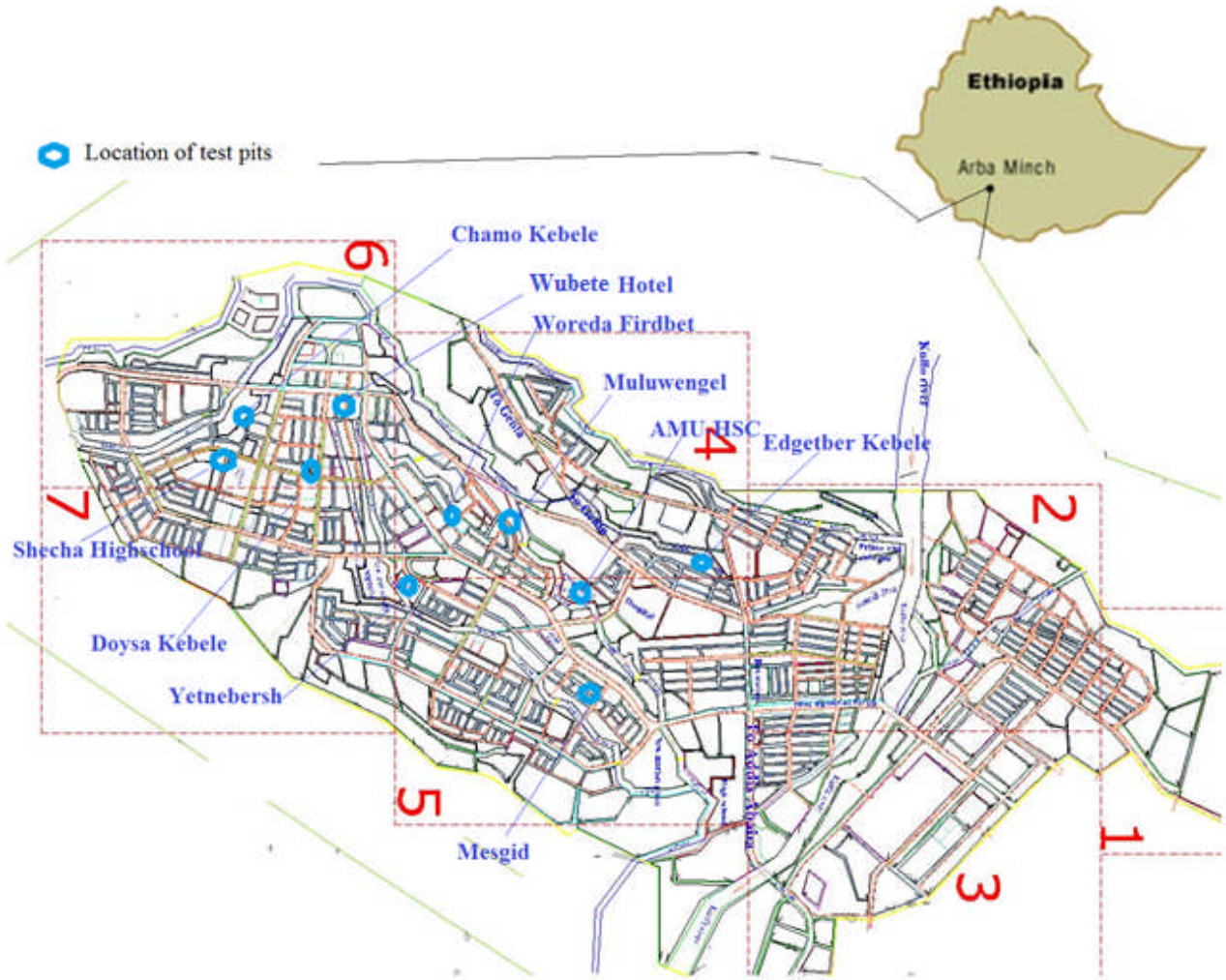

Figure 1.1 Location of test pits

1.5. Organization of the Thesis

The thesis is organized into five Chapters. The first Chapter is about the current problems associated with expansive soils, motivation and objectives, study area description and scope of the thesis. A compressive literature review on the origin, formation, mineralogy and different characteristics of expansive soils and the concept of unsaturated soil mechanics are presented in Chapter two. In the third Chapter, the tests that were made on the samples and the results obtained from the tests are jotted down. The discussion on the results obtained from the tests is given in Chapter four and the last Chapter is devoted to conclusion and recommendations.

2. LITERATURE REVIEW

2.1. General

2.1.1. Genesis of Expansive Soils

The origin of expansive soils is related to a complex combination of conditions and processes that result in the formation of clay minerals having a particular chemical makeup which, when in contact with water, will expand. Variations in the conditions and processes may also form other clay minerals, most of which are non-expansive. The conditions and processes which determine the clay mineralogy include composition of the parent material and degree of physical and chemical weathering to which the materials are subjected (Chen, 1988).

2.1.2. Parent Material

The parent material associated with expansive soils may be classified in to two groups. The first group comprises the basic igneous rocks, which are low in silica, generally about 45% to 25%, such as basalt, dolerite sills and dykes, gabbros, etc., where feldspar, amphiboles, biotitic, olivine and pyroxene minerals of the parent rock decomposes to form Montmorillonite. The second group includes sedimentary rocks like shales and claystone, and limestone and marls rich in magnesium that contain Montmorillonite, and break down physically to form expansive soils. There are indications that confirm that the expansive soils of Ethiopia are derived from both groups (Teferra, 2009; Chen, 1988).

2.1.3. Weathering and Climate

The weathering process by which clay is formed includes physical, biological and chemical process. The most important weathering process responsible for the formation of Montmorillonite is the chemical weathering, which include hydrolysis, hydration, oxidation, carbonation and solution, of parent rock mineral which generally consists of ferromagnesium mineral, calcic feldspars, volcanic glass, volcanic rocks and volcanic ash. The formation is aided in alkaline environment, presence of magnesium ion and lack of leaching. Such condition is favourable in semi-arid regions with relatively low rainfall or seasonal moderate rainfall particularly where evaporation exceeds precipitation. Under these conditions enough water is available for the alteration process but the accumulated cations will not be removed by rainwater.

2.1.4. Mineralogical Structure

There are two fundamental molecular structures as the basic units of the lattice structure of clay soils. These are the silica tetrahedron and the alumina octahedron. The silica tetrahedron consists of a silicon atom surrounded tetrahedrally by oxygen ions. The alumina octahedron consists of an aluminium atom surrounded octahedrally by six oxygen ions. There are valency imbalances in both units, resulting in net negative charges. The basic units, therefore, do not exist in isolation but combine to form sheet structures. When each oxygen atom is shared by two tetrahedral, a plate- shaped layer is formed. Similarly, when each aluminium atom is shared by two octahedrons, a sheet is formed. The silica sheets and the aluminium sheets combine to form the basic structural units of the clay particles. Various clay minerals differ in the stacking configuration (Murray, 2007; Craig, 2004).

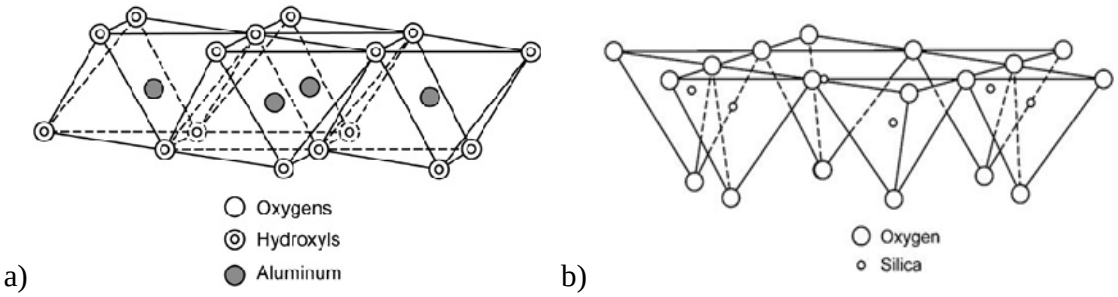

a) b)

Figure 2-1 Diagrammatic sketch of a) Octahedral sheet; b) Tetrahedral sheet (Murray, 2007)

The tetrahedral sheet (also called silica sheet) retains a net negative charge but the octahedral sheet (gibbsite sheet) is electrically neutral. Silicon and aluminium may be partially replaced by other elements, this being known as isomorphous substitution, resulting in further charge imbalance. The sheet structures are represented symbolically in Figure 2.2(a). Layer structures then form by the bonding of a silica sheet with either one or two gibbsite sheets. Clay mineral particles consist of stacks of these layers, with different forms of bonding between the layers. The structures of the principal clay minerals are depicted in Figure 2.2 (Craig, 2004).

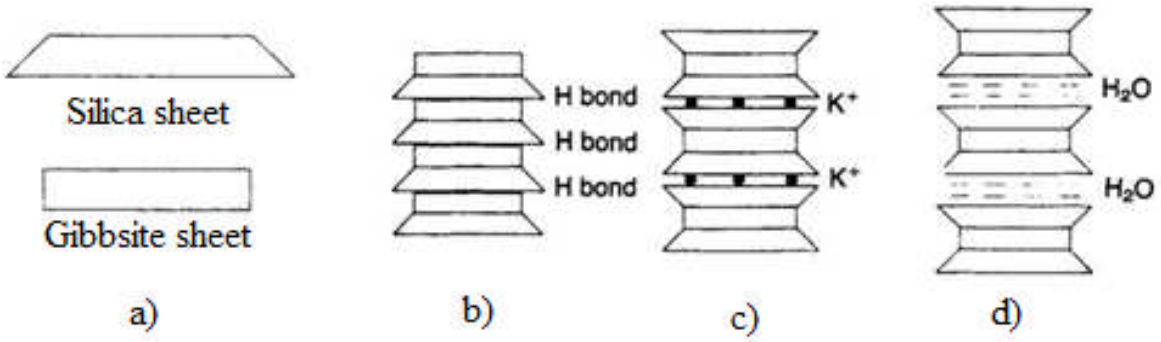

Figure 2-2 Principal Clay minerals: a) Symbolic representation of the sheet structures; b) Kaolinite; c) Illite and d) Montimorillonite (Craig, 2004)

Most clay mineral particles are of 'plate-like' form having a high specific surface (i.e. a high surface area to mass ratio) with the result that their structure is influenced significantly by surface forces. Long 'needle-shaped' particles can also occur but are comparatively rare (Craig, 2004).

2.1.5. Distribution of expansive soils

Damages to structures from the swell of foundation soils due to change in moisture conditions are common problems that occur frequently in many parts of the world – both in temperate and tropical countries since identified in the latter part of 1930's (Teklu, 2003). Among the countries that reported the problem include U.S.A., Canada, Cuba, Argentina, Australia, Spain, Burma, India, Israel, Iran, Saudi Arabia, Mexico, Turkey, Venezuela, South Africa, Kenya, Ghana, Morocco, Zimbabwe, Ethiopia, Nigeria and a number of other countries (Al-Rawas and Goosen, 2006; Chen, 1988; Teklu, 2003; Teferra and Leikun, 1999). The distribution of this problematic soil in Africa is depicted in Figure 2.3.

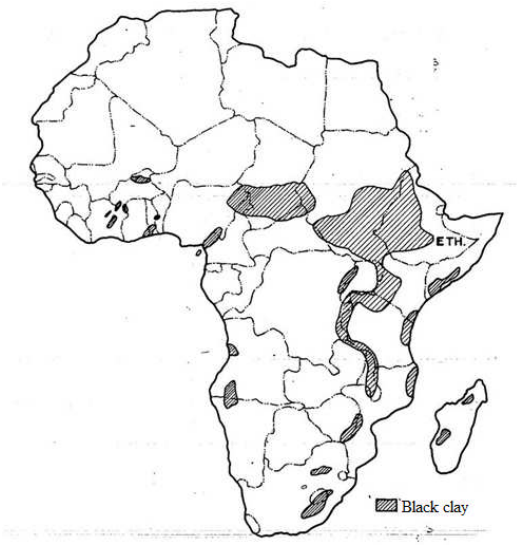

Figure 2-3 Distribution of expansive soils in Africa (Teferra and Leikun, 1999).

2.2.Identification and Classification of Expansive Soils

A major concern in geotechnical engineering is identification of expansive soils, either in the field or laboratory, and estimation of their swelling magnitudes when subjected to changes in environment so that problems posed by them can be counteracted (Al-Rawas and Goosen, 2006).

2.2.1. Field Identification

It is easy to recognize expansive soils in the field during either dry or wet seasons. Their color varies from dark grey to black. During dry seasons, shrinkage cracks are visible on the ground surface with the maximum width of these cracks reaching up to 20 mm or more and they travel deep into the ground. A lump of dry black cotton soil requires a hammer to break. A shiny surface is easily obtained when a partially dry piece of the soil is polished with a smooth object such as the top of a finger nail. During rainy seasons, these soils become very sticky and very difficult to traverse. Appearance of cracking in the nearby structures is also indicative (Murthy, 2003; Teklu, 2003).

2.2.2. Laboratory Identification

As stated in Al-Rawas and Goosen (2006); Chen (1988); Teklu (2003); Tilahun (2007), shrink–swell behavior can be best predicted by examining a combination of physical, chemical, and

mineralogical soil properties. To achieve this, many tests and method have been developed. These include mineralogical, direct and indirect identification techniques.

The mineralogical identification methods, such as : X-ray diffraction, Differential thermal analysis, Dye absorption, Electron microscope, Base exchange capacity, etc, use the mineralogy of clay particles such as characteristic crystal dimensions, characteristic reaction to heat treatment, size and shape of clay particles and change deficiency and surface activity of clay particle. These properties are fundamental factors controlling expansive soil behavior. However, they are not suitable for routine testing as they are time consuming, require expensive test equipment and, the results are interpreted by specially trained technicians (Chen, 1988; Teklu, 2003).

Indirect methods involve the use of indirect information from soil index and physical properties and classification schemes to estimate shrink–swell potential. These include Index Property Tests, Cation Exchange Capacity (CEC), and Potential Volume Change (PVC) test. None of the indirect methods should be used independently.

Grain Size Analysis, Atterberg Limit (Liquid Limit, Plastic Limit and Shrinkage Limit) and Free Swell tests are some, among the routinely conducted index property tests. Since the LL and swelling of clays both depend on the amount of water a clay tries to imbibe, it is not surprising that they are related (Chen, 1988; Ulusay, 2002). While it may be true that high swelling soil will manifest high index property, the converse is not true (Chen, 1988).

The grain size analysis helps to determine the amount of colloidal sized particles existing in a soil. The term colloid describes a particle whose behavior is controlled by surface force (i.e. electrostatic and adsorptive force) rather than by gravitational force and smaller than 0.001 mm in diameter. These colloidal particles greatly influence the plasticity characteristics and volume change behavior of the soil. In this identification method, Atterberg limit and clay contents are combined to define activity.

The direct method provides the actual physical measurement of swelling that the soil undergoes as the moisture content changes and hence a convenient and dependable method for a practicing

engineer. It can be done by the use of a conventional one-dimensional Consolidometer which is available in most soil mechanics laboratories.

2.2.3. Classification of Expansive soils

Soil classification is an important aspect of laboratory test, which tells the characteristic of the soil under interest. There are a number of classification systems based on identification tests. Among these, the Unified Soil Classification System (USCS) and the American Association of State Highway Transport Officials (AASHTO) method make use the liquid limit and plasticity index of the soil. Geotechnical engineers generally prefer the USCS while the AASHTO classification is common in state and country highway departments (Das, 2002). There are also other classification methods specifically proposed for expansive soils, one of them is the single index method. However, the use of single index method of classification alone may lead to wrong conclusion (Chen, 1988; Teklu, 2003).

2.3. Mechanics of Swelling in Expansive soils

The mechanism of swelling in expansive soil is complex and is influenced by a number of factors. Expansion is the result of change in the sol water system that disturbs the internal force equilibrium. There must be a potential gradient, which can cause water migration and a continuous passage through which water transfer can take place to cause volumetric expansion. Fractures and fissures, shrinkage cracks, capillary force, vapor transfer, thermal gradients, etc are some of the sources that cause moisture migration and swelling on expansive soils (Chen, 1988).

In general, the movement of expansive soil occurs in an uneven pattern and the resulting expansion is a magnitude that cannot be predicted by the classical elastic or plastic theory (Nelson and Miller, 1992). However, the swelling behavior can be basically related to the combined effect of interacting factors that can be grouped into: (a) local geology; (b) engineering properties and; (c) local environment of deposition. The main geological factors include the rock type and age as related to the type and amount of clay minerals, type and amount of cementing material and the soil particles arrangement. The engineering factors include the moisture content, Atterberge limits, and the dry density. The environmental factors include the confining pressure, type and degree of weathering as related to the amount of clay fraction, initial water content

(Nelson and Miller, 1992) and water. The swelling potential is related to the geological and engineering factors while the amount and rate of swelling are controlled by environmental conditions (Sabtan, 2005). By far the most important element and of most concern to the practicing engineer is the effect of water on expansive soil (Chen, 1988).

Thickness and location of potentially expansive layers in a profile considerably influence potential movement. Greatest movement will occur in profiles that have expansive clays extending below the active zone. Less movement will occur if expansive soil is overlain by non-expansive material or have got shallow depths. Water contents in the upper few meters of the expansive soil profile are affected by environmental factors and generally called Zone of seasonal variation or active zone. If one measures the water content of the expansive soils with respect to depth during dry and wet seasons, the variation is similar to the one shown in Figure 2.4 (Chen, 1988).

During dry seasons, the natural water content is practically zero on the surface and the volume of the soil reaches the shrinkage limit due to loss of moisture content in the soil near the ground surface in response to evaporation and transpiration (Murthy, 2003). Hence, the moisture content will increase with depth. However, the influence of evaporation decreases with depth and at some depth, D_{us}, beyond which the moisture content equilibrium remains almost constant. The maximum depth of D_{us} is equal to the depth of the water table, and the minimum depth is equal to the depth of the seasonal moisture contents fluctuation, D_s. During wet months with heavier precipitation and higher humidity, the moisture content of near surface soil increases and the moisture profile represented by curve 2 alters its shape to curve 3 (Chen, 1988).

The watering of lawns, planting of trees and shrubs, discharge of roof drains, formation of drainage channels and swales, and the possibility of utility line leakage will all increase the value of D_s. When areas are covered by structures such as buildings, pavements, sidewalks or aprons, evaporation is blocked or partially retarded. The moisture content beneath the covered area increases due to gravitational migration, capillary action, vapor, and liquid thermal transfer and, in the course of several years, the depth of seasonal moisture content fluctuation D_s can approach to the depth of desiccation D_{us} (Chen, 1988).

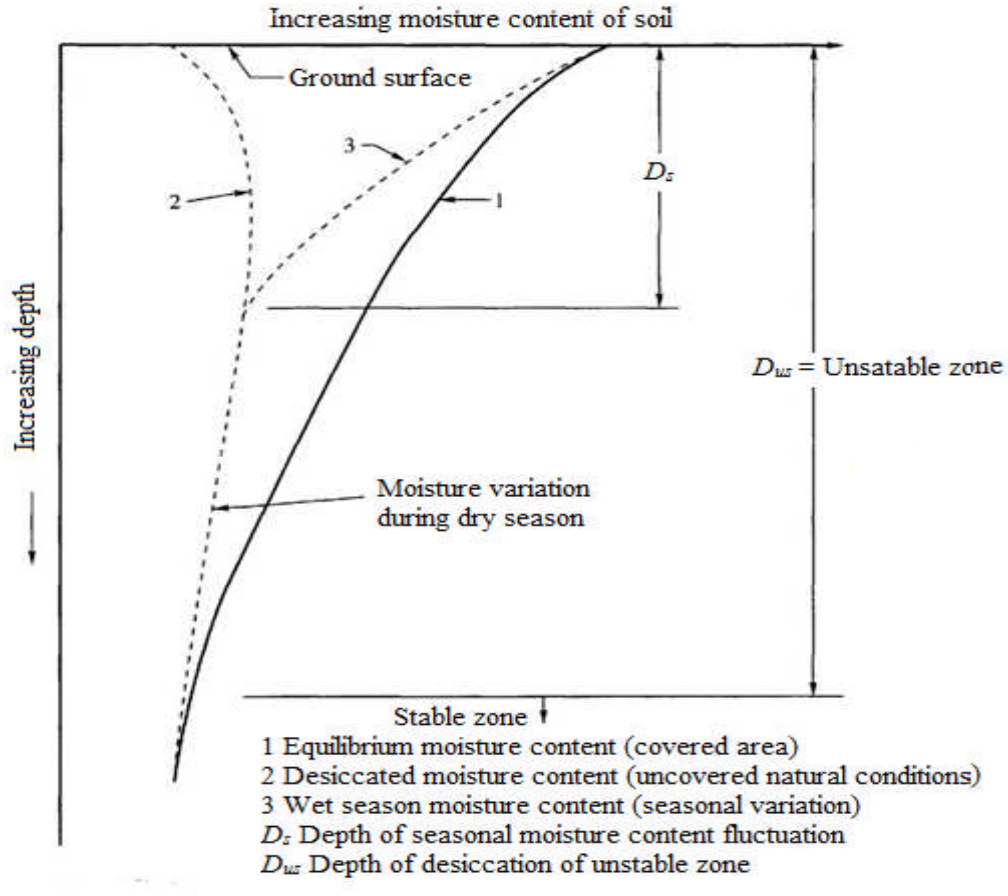

Figure 2-4 Moisture content variations with depth below ground surface (Chen, 1988).

2.4. Swelling Pressure Predictive Models

Since the laboratory-swelling test is a difficult and an expensive process for practicing engineers and small builders, empirical methods that make use of the routine index and/or physical properties have got increasing popularity (Al-Rawas and Goosen, 2006). However, each empirical equation need to be applied to the site for which they are developed in order to give fair evaluation as the swell potential is dependent on the geology, environmental factors, soil characteristics and many other factors, which vary from place to place (Tilahun, 2007). The following are developed in our country:

i) Daniel Teklu (2003) based on Addis Ababa expansive soils proposed:

$$LogP_s = -5.00 - 0.000206LL + 0.003477PI + 0.005827\gamma_d \quad (2.1)$$

$$LogP_s = -9.384 + 0.0278\omega + 0.006307PI + 0.008359\gamma_d \quad (2.2)$$

Where P_s is the swelling pressure in kPa; ω, LL, and PI are the natural moisture content, liquid limit and plastic index, respectively in percentage; and γ_d is the dry density in kg/m^3.

ii) Dagmawe Nigussie (2007) suggested the following equation from index tests performed on Bahir Dar expansive soils:

$$LogP_s = 7.042 - 1.926\gamma_{dry} - 0.046\omega - 0.609A_c \quad (2.3)$$

Where, γ_{dry} is in gm /cc; is natural moisture content in % and P_s the swelling pressure in kPa.

Komornik and David (1969) ; Vijayvergiya and Ghazzaly, (1973) and Nayak and Christensen (1974) based on experimental data, proposed relationships for swell potential and swelling pressure involving both placement conditions and index properties. Though these were developed for temperate climatic condition, their validity has been verified in the African tropical black clays like Tanzanian soils and Gebrehiwot (2003) has used the equations as there is a similarity of prevailing soil conditions in Tanzanian and the East African occurrences, like the Ethiopian (Lyone Associates, in Gebrehiwot, 2003). The relationships have been selected for their simplicity, wide acceptance and practical significance to field applications (Gebrehiwot, 2003) .

Komornik and David (1969) proposed the following correlation for swelling pressure of undisturbed clay:

$$LogP_s = -2.132 + 0.0208\omega_L + 0.000665\gamma_d - 0.0269\omega i \quad (2.4)$$

Where, P_s is the swelling pressure in kg/cm^2, ω_L is the liquid limit in %, γ_d is the dry density in kg/m^3, and $_i$ the initial moisture content in %.

Vijayvergiya and Ghazzaly (1973) proposed the following correlations for swelling pressure of undisturbed samples tested under a surcharge of 10 kPa.

$$LogP_s = \frac{1}{19.5}(\gamma_d + 0.65\omega_L - 139.5) \quad (2.5)$$

Where, P_s is the swell pressure in tons/ft^2, γ_d is the dry density of the soil in lb/ft^3, ω_L is the liquid limit in %.

Nayak and Christensen (1974) gave statistical relationships for swelling pressure as:

$$P_s = 2.50 * 10^{-1} (PI)^{1.12} * \frac{C^2}{\omega_i^2} + 25 \quad (2.6)$$

Where, P_s is the swelling pressure (kN/m^2), PI is the plasticity index, C is the clay content, and ω_i is the initial water content (%).

2.5. Unsaturated Soils

In tropical and arid regions, even in temperate climatic zones soils exist above the ground water table and remain partially saturated/ unsaturated. Tropical and arid regions of the world comprise more than one-third of the earth's surface. Soils in these regions are dry and desiccated near the ground surface. These conditions may exist to a considerable depth below the ground surface. Expansive soils are residual soils generally located in these regions and are usually in an unsaturated state (İkizler et.al, 2007; Murthy, 2007). The compacted soils used in several engineering constructions, such as earth dams, highways, embankments, and airport runways, are unsaturated soils.

2.5.1. Emergence of Unsaturated Soil Mechanics

On the course of trying to eliminate the excessive financial losses due to lack of correct understanding of the behavior of expansive soils, seven conferences under the name ’International Conference on Expansive Soils’ took place in 1965, 1969, 1973, 1980, 1984, 1987 and 1992. Though the main aim of these conferences was to close the knowledge gap in the expansive soil arena of foundation engineering, they gave birth to ‘Unsaturated soil mechanics’ as an independent science with extended rules as compared to classical soil mechanics. This is because, in 1995, the focus of these conferences shifted slightly toward the broader topic of unsaturated soils. Although the attention given to truly expansive soils may seem to have diminished, active research is still recorded in many parts of the world (Stephen et.al, 2005). Thus, it can be said that expansive soils have been the subject, if not the driving force, of

unsaturated soil research since the early stages in the formulation of unsaturated soil mechanics principles (Lu and Likos, 2004). Further international conferences held under the name 'Unsaturated Soil' in 1995, 1998, 2002 and 2006 has led expansive soil investigations inseparable to studying unsaturated soil mechanics (Abed, 2008).

2.5.2. Concept of Soil Suction

Soil suction, more often used in expansive soil studies, is a parameter describing the state of the soil and indicates the intensity with which it will attract water (Chen, 1988). It is commonly referred to as the free energy state of soil water. The free energy of the soil water can be measured in terms of the partial vapor pressure of the soil water. The theoretical concept of suction was developed in early 1900's and this concept was first applied to unsaturated soils by United States Road Research Laboratory, now known as United States Transport Research Laboratory (Chakraborty, 2009).

The soil suction as quantified in terms of relative humidity is commonly called "total suction (h_t)"; which is the total free energy of the soil water determined as the ratio of the partial pressure of the water vapour in equilibrium with a solution identical in composition to the soil water, to the partial pressure of the water vapour in equilibrium with a pool of free pure water. It has two components (i.e., matric suction (h_m) and osmotic suction (π)).

$$h_t = h_m + \pi \tag{2.7}$$

Matric suction (h_m) is the component of free energy of the soil water, which is determined as the ratio of partial pressure of the water vapour in equilibrium with the soil water, relative to partial pressure of the water vapour in equilibrium with a solution identical in composition with a pool of soil water (Fredulnd and Rahardjo, 1993; Allah, 2009). It is usually defined as the difference between pore-air pressure (u_a) and pore-water pressure (u_w) in the soil.

Osmotic suction (π) is a reduction in relative humidity in a pore, due to the presence of dissolved salts in pore water. For most practical geotechnical engineering applications, chemistry of pore fluids in the soil is not changed and soil–water content varies within a range in which concentrations of pore fluids are not altered significantly, and so osmotic suction appears not to

be sensitive to changes in soil–water content (Chen, 1988; Ng and Menizies, 2007). Therefore, for most geotechnical problems involving unsaturated soils, matric suction changes can be substituted for total suction changes, and vice versa. However, in the case where the salt content of the soil is altered by chemical contamination, it is necessary to consider osmotic suction as part of the stress state (Fredlund and Rahardjo, 1993).

2.5.3. Stress State Variables for Unsaturated Soil

Many geotechnical problems involving saturated soils have been successfully addressed in the conventional soil mechanics with the help of effective stress concept as all mechanical aspects (i.e., the volume change, seepage and shear strength behavior) of a saturated soil are governed by the effective stress. For such a soil, one stress state variable is enough to describe the behavior of two phases (solid and fluid/or gas) of the soil mass. The stress state variable σ` is defined as σ` = σ − u_w, where σ` is the effective stress, σ is the total stress, and u_w is the pore-water pressure (Terzaghi, 1943).

Unsaturated soil is normally considered as a three-phase system, i.e., solid, gas (air), and fluid (water). In 1977, Fredlund and Morgenstern added the contractile skin as a fourth phase (Figure 2.5) and these four phases were used by these two authors in the stress analysis of unsaturated soil on the basis of continuum mechanics. Several authors tried to define a single stress state variable for unsaturated soil but soil properties were involved in the proposed equations. State variables used to describe the state of the stress have to be independent of soil properties (Fredlund and Rahardjo, 1993; Ng and Menizies, 2007). Bishop in 1959 proposed the following single effective stress equation for unsaturated soil:

$$\sigma' = (\sigma - u_a) + \chi(u_a - u_w) \tag{2.8}$$

where σ` is the effective stress, σ is total stress and χ (effective stress parameter) is a parameter that depends on the degree of saturation and usually assumes a value of unity for saturated soil and zero for a dry soil, but in rare instances, may exceed one (Blight, 1997). In 1961, Bishop and Donald in Fredlund and Rahardjo (1993) performed a set of triaxial shear tests on unsaturated silt where the total stress (i.e., cell pressure), pore-air pressure, and pore-water pressure were varied

by equal amount keeping ($\sigma_3 - u_a$) and ($u_a - u_w$) constant. The result of these tests lent credibility to the use of ($\sigma_3 - u_a$) and ($u_a - u_w$) as valid stress state variables for this type of test.

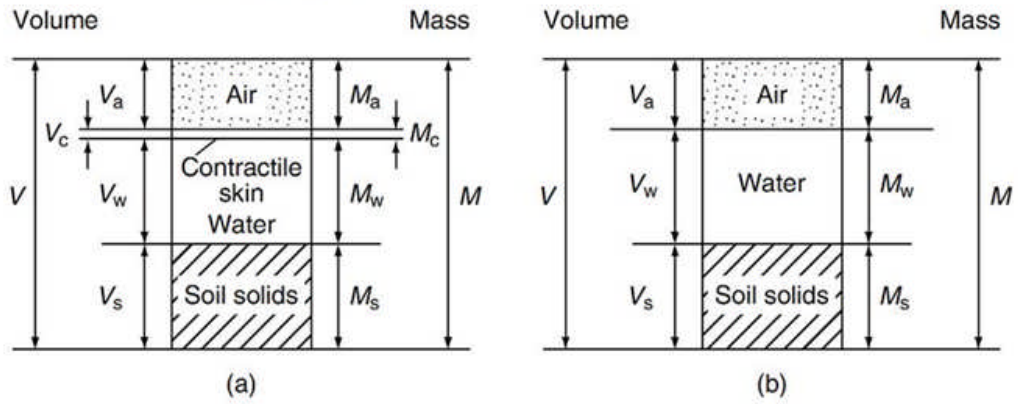

Figure 2-5 Rigorous and simplified phase diagrams for an unsaturated soil. (a) Rigorous four-phase unsaturated soil system; (b) simplified three phase diagram (Fredlund and Rahardjo, 1993).

Fredlund and Rahardjo (1993) discussed the stress state variables controlling the behavior of unsaturated soil. They stated that the stress state variables have to be created from the individual force components acting on the solid, water and air phases, and the air-water contractile skin. The proposed variables are the net stress ($\sigma - u_a$) and the matric suction ($u_a - u_w$). In the same work, Fredlund and Rahardjo (1993) validated the concept of stress state variables by a set of tests. In these tests it has been proven that changing the air, water, and the total pressures causes no changes in the state of the soil as long as the state variables remain constant. Figure 2.6 shows the stress state in an unsaturated soil element. By convention, positive normal stresses (shown) indicate compression on the cubic element. Negative normal stresses indicate tension. Thus, following the multiphase continuum mechanics methodology, each of these independent stress variables in three – dimensional space can be represented by two independent stress tensors as follows:

$$\begin{bmatrix} \sigma_x - u_a & \tau_{xy} & \tau_{xz} \\ \tau_{yx} & \sigma_y - u_a & \tau_{yz} \\ \tau_{zx} & \tau_{zy} & \sigma_z - u_a \end{bmatrix}$$

And $$\begin{bmatrix} u_a - u_w & 0 & 0 \\ 0 & u_a - u_w & 0 \\ 0 & 0 & u_a - u_w \end{bmatrix}$$

In a case where unsaturated soil approaches saturation as the degree of saturation S, approaches 100%, the pore-water pressure, u_w, comes close to the pore-air pressure, u_a, and the matric suction term, (u_a - u_w), goes towards zero with only the first stress tensor retained for a saturated soil as the second stress tensor disappears due to vanishing matric suction. On the other side, as a soil becomes extremely dry, even if matric suction remains a stress state variable, it may not be required in describing the behavior of the soil for its change may no longer produce any significant changes in mechanical properties. Therefore, only the first stress tensor with the net normal stress ($\sigma - u_a$) may be required, even though it may be necessary to consider matric suction as a stress state variable when examining the volume increase or swelling of a dry soil (Fredlund and Rahardjo, 1993; Ng and Menizies, 2007).

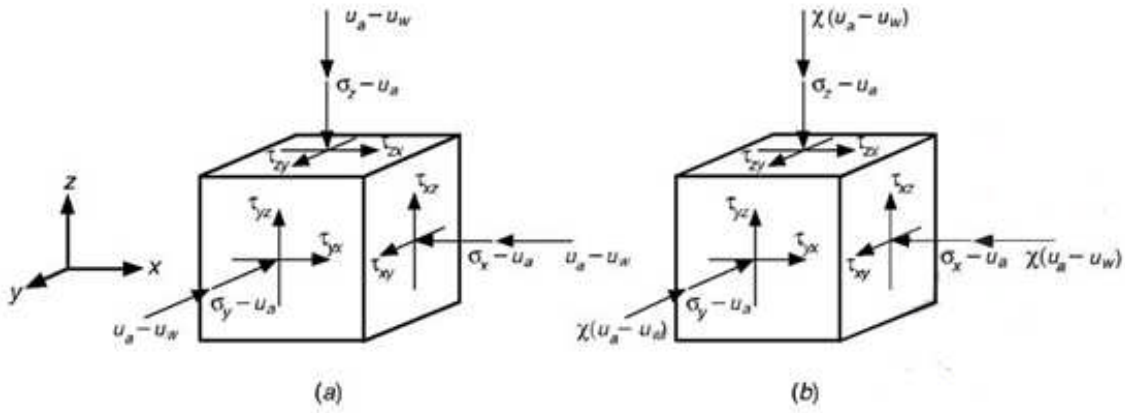

Figure 2-6 Normal and shear stresses in unsaturated soil element: (a) independent stress state variable approach; (b) following Bishop's effective stress approach (eqn. 2.8) (Lu and Likos, 2004)

2.5.4. Shear Strength of Unsaturated Soil

Shear strength of unsaturated soil is an important engineering property in various geotechnical designs for addressing numerous engineering problems like bearing capacity, slope stability, lateral earth pressure, pavement design, and foundation design, where stability of a given soil mass under load is of concern. The shear strength of a soil can be related to the stress state in the soil. There is a general agreement on the use of the net stress ($\sigma - u_a$) and the matric suction ($u_a -$

u_w) as a stress state variables for unsaturated soils (Fredlund and Rahardjo, 1993), with the matric suction providing additional shear strength component which normally is referred to as apparent cohesion.

2.5.4.1. **Theory of Shear Strength of Unsaturated Soil**

The shear strength of soil, whether saturated or unsaturated, may be defined as the maximum internal resistance per unit area the soil is capable of sustaining along the failure plane under external or internal stress loading. The use of effective stresses with the Mohr-Coulomb failure criterion has proven to be satisfactory in engineering practice associated with saturated soils, which defines the shear strength in terms of the material variable ϕ' and c' and the stress state variable effective stress (Terzaghi, 1943) as

$$\tau_{ff} = c' + (\sigma_f - u_w)_f \tan\phi' \qquad (2.9)$$

Where τ_{ff} = shear stress on the failure plane at failure

c' = effective cohesion, which is the shear strength intercept when the effective normal stress is equal to zero.

$(\sigma_f - u_w)_f$ = effective normal stress on the failure plane at failure

σ_{ff} = total normal stress on the failure plane at failure

u_w = pore-water pressure at failure

ϕ' = effective angle of internal friction

The above equation defines a straight line and is commonly referred to as a Mohr-coulomb *failure envelope* because any combination of effective normal stress and shear stress defined by the points along the line corresponds to a failure condition. Accordingly, the shear stress along the failure envelope describes the shear strength of the soil under the corresponding effective normal stress.

Fredlund and Rahardjo (1993) proposed the following equation to explain the shear strength of unsaturated soils as an extension of the shear strength equation of saturated soil:

$$\tau_{ff} = c' + (\sigma_f - u_a)_f \tan\phi' + (u_a - u_w)_f \tan\phi^b \qquad (2.10)$$

Where τ_{ff} =shear stress on the failure plane at failure

c'= intercept of the "extended "Mohr –Coulomb failure envelope on the shear stress axis where the net normal stress and the matric suction at failure are equal to zero

$(\sigma_f - u_a)_f$ =net normal stress state on the failure plane at failure

u_{af}=pore –air pressure on the failure plane at failure

ϕ'=angle of internal friction associated with the net normal stress state variable, $(\sigma_f - u_a)_f$

$(u_a - u_w)_f$ =matric suction on the failure plane at failure

ϕ^b =angle indicating the rate of increase in shear strength relative to the matric suction

The above equation reverts to the equation for a saturated soil when the matric suction vanishes as the soil approaches saturation. The failure envelope represented by this equation is a planar surface in the three dimensional space of the stress state variables; the net normal stress ($\sigma - u_a$) and the matric suction ($u_a - u_w$) as abscissas and the shear stress, τ as an ordinate. Figure 2.7 shows the Mohr-Coulomb failure envelope for saturated soil and the extended failure surface for unsaturated soil. In Figure 2.7 (a), the state of stress described by Mohr's circle A is in an elastic state – the soil element remains stable and that described by Mohr's circle B represents a failure condition (Lu and Likos, 2004).

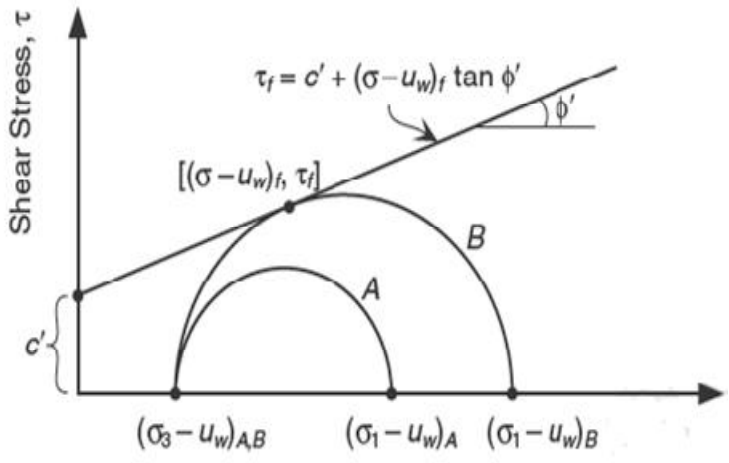

a)

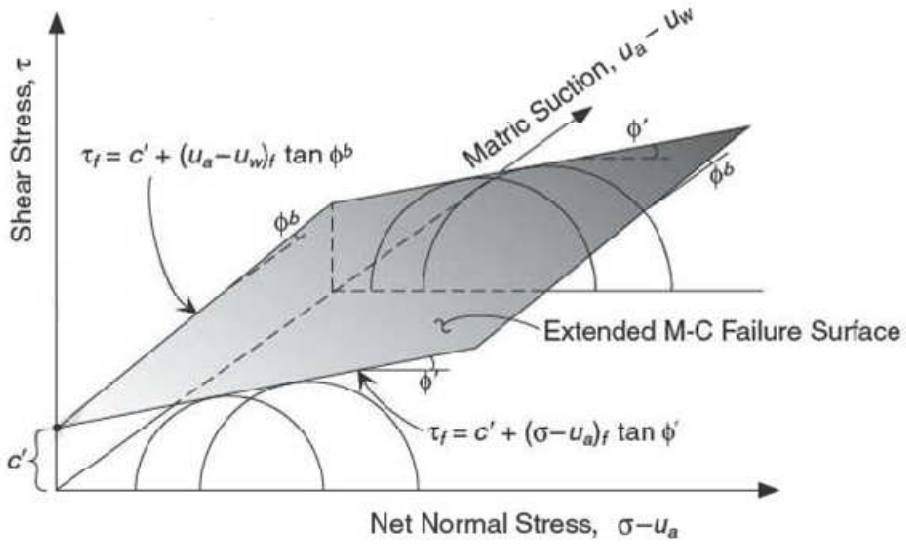

b)

Figure 2-7 Mohr-Coulomb criterion: (a) failure envelope for saturated soil; (b) failure surface for unsaturated soil (Lu and Likos, 2004)

2.5.4.2. **Laboratory Measurement of Shear Parameters for Unsaturated Soil**

In unsaturated soil testing, conventional triaxial and direct shear test equipments require adjustment prior to use as it is essential to control the pore-air pressure within the sample independently of the pore-water pressure. This can be achieved by using ceramic discs which in the case of full saturation enable water to pass but prevent air from passing through it. This value of air pressure at which the air can pass through the ceramic disc is called the air entry value of the disc (AEV). At this point, air enters the water compartment, which no longer maintains continuity between the pore-water and the water in the measuring system. The measuring system then becomes filled with air bubbles. Ceramic discs are available with deferent diameters, thicknesses, and air-entry values (Fredlund and Rahardjo, 1993).

The other issue of concern is how to apply high values of matric suction (i.e. how to apply high negative pore-water pressure within the soil specimen). This can also be overcome by using the axis translation technique with modification applied to the conventional soil testing equipments. The term axis translation refers to the practice of elevating pore air pressure in unsaturated soil while maintaining the pore water pressure at a measurable reference value, typically

atmospheric. As such, the matric suction variable may be controlled over a range far greater than the cavitation limit for water under negative pressure. The origin of reference, or "axis" for the matric suction variable is "translated" from the condition of atmospheric air pressure and negative water pressure to the condition of atmospheric water pressure and positive air pressure (Lu and Likos, 2004). The main amendment on testing equipments is to provide ceramic discs to facilitate the application of the matric suction. Encompassing this improvement, the modified direct shear devices and triaxial apparatuses are being in use to measure the shear parameter of unsaturated soil (Fredlund and Rahardjo, 1993). As part of this work, only triaxial tests are presented and for the modified direct shear testing details, interested one is directed to Fredlund and Rahardjo, (1993).

2.5.4.2.1. Triaxial Tests

Various triaxial test methods are defined on the bases of drainage conditions during the application of the confining pressure, σ_3, and the drainage condition upon the application of deviator stress, (σ_1-σ_3) through the loading ram in contact with the top of a cylindrical soil specimen enclosed in a rubber membrane placed in the triaxial cell filled with water. The methods, listed in Table 2.1, are usually given a two word designation or abbreviated to a two-letter symbol with the first letter indicating the drainage condition prior to shear whereas the latter referring to the condition during shear (Fredlund and Rahardjo, 1993).

Table 2.1 Common triaxial tests for unsaturated soil (Abed, 2008)

Test	Consolidation phase	Shear phase
Consolidated Drained or *CD* test	All-around confining net stress ($\sigma_3 - u_a$) is applied. The consolidation phase ends when the sample reaches equilibrium. The equilibrium means that there is no further tendency to change the total volume or water flow out of the sample.	The vertical net ($\sigma_1 - u_a$) is increased till failure. Valves A and C are always open.
Constant Water content test or *CW* test	Similar to the *Consolidated Drained test*	The sample is sheared with undrained water phase and drained air phase. This implies that valve C is open

		but valves *A* and *B* are closed.
Consolidated Undrained or *CU* test	Similar to the *Consolidated Drained test*	The sample is sheared with undrained conditions for both water and air phases. Valves A, B and *C* are always closed.
Unconsolidated Undrained or *UU* test	There is no Consolidation phase	The initial suction or water content is kept constant during this kind of tests. The conventional triaxial apparatus can be used for this test.
Unconfined Compression or *UC* test	There is no Consolidation phase	Similar to the *Unconsolidated Undrained test* but without confining pressure.

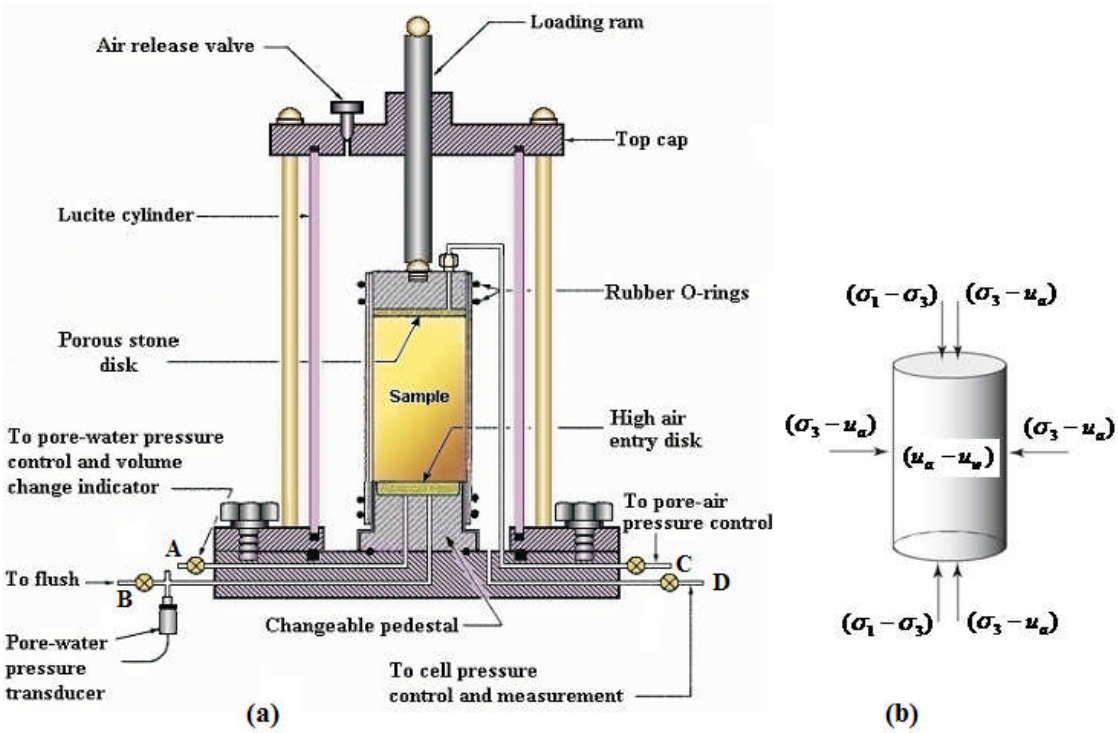

Figure 2-8 (a) Longitudinal section of Modified triaxial equipment for testing of unsaturated soils after Fredulend and Rahardjo (1993); (b) Applied stresses during the test

The valves A, C and D in Figure 2.8 (a) are used for applying pore water pressure and pore air pressure on the sample. By closing or opening them one controls the type of the test being conducted. For the current work, due to the very low permeability characteristic of the soil under study and the long time duration needed for unsaturated testing, Consolidated Undrained test will be presented and for the rest, the interested reader is referred to Fredlund and Rahardjo (1993) for further information.

2.5.4.2.1.1. Consolidated Undrained (CU) Test

In this method of triaxial testing, the soil specimen is consolidated first and then sheared by increasing the deviator stress $(\sigma_1 - \sigma_3)$ until failure; maintaining the pore- air and pore -water under undrained conditions during shear. The developing excess pore- air and pore- water pressures should be measured during the shearing process. The net confining pressure, $(\sigma_3 - u_a)$, and the matric suction, $(u_a - u_w)$, are altered throughout the test due to the changing pore- air and pore-water pressures. At failure, the magnitude of the net major and minor principal stresses and the matric suction are a function of the pore –pressures.

A typical stress path for a consolidated undrained test is illustrated in Fig 2.9. The stress state at the end of consolidation is represented by point A where the net confining pressure is $(\sigma_3 - u_a)$ and the matric suction is $(u_a - u_w)$. Shear causes stress state to move from point A to point B, along stress path $\overline{AB}$. The stress state at failure is represented by stress point B, corresponding to a different net confining pressure and matric suction from those associated with stress point A.

As indicated in the drawing, the pore air pressure is assumed to increase continuously during shear. This causes the net confining pressure to decrease [i.e. $(\sigma_3 - u_a)_f < (\sigma_3 - u_a)$]. The matric suction is also assumed to decrease continuously [i.e $(u_a - u_w)_f < (u_a - u_w)$]. The failure envelope is tangent to Mohr circle at failure (e.g at stress point c)and inclined at an angle of ϕ' with respect to the $(\sigma - u_a)$ axis. The failure envelope intersects the shear strength verses

$(u_a - u_w)$ plane at a cohesion intercept ,c. The intersection line joining the cohesion intercepts produced by tests at different matric suctions gives the angle, ϕ^b (Fredlund and Rahardjo, 1993).

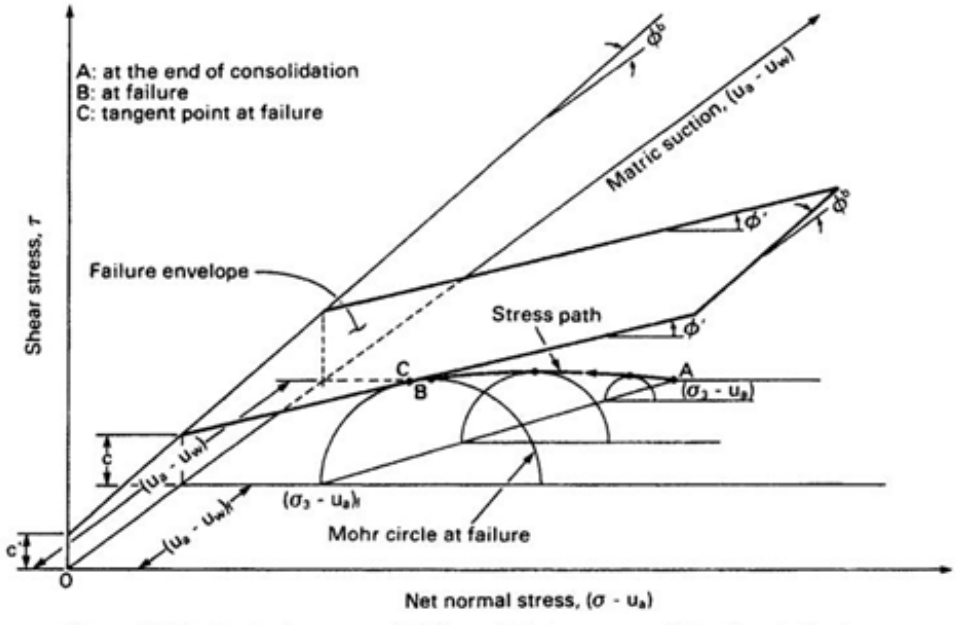

Figure 2-9 Typical stress path followed during consolidated undrained test (Fredlund and Rahardjo, 1993).

2.5.5. Previous works on expansive soils

The shear strength characteristics of an expansive silty clay from china were studied by Zhan and Ng (2006) with suction controlled direct shear test on both compacted and natural specimens. The contribution of suction to shear strength and the variation of $\varnothing^b$ angles with matric suction for their test samples are replicated in Figure 2-10 and Figure 2-11, respectively.

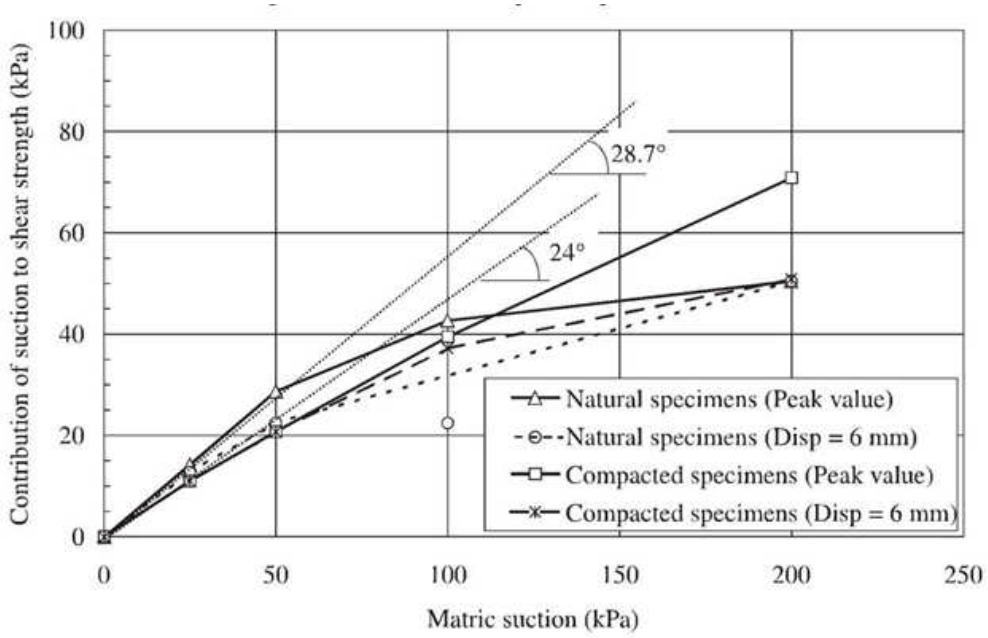

Figure 2-10 Contribution of suction to shear strength for natural and compacted specimens (Zhan and Ng, 2006).

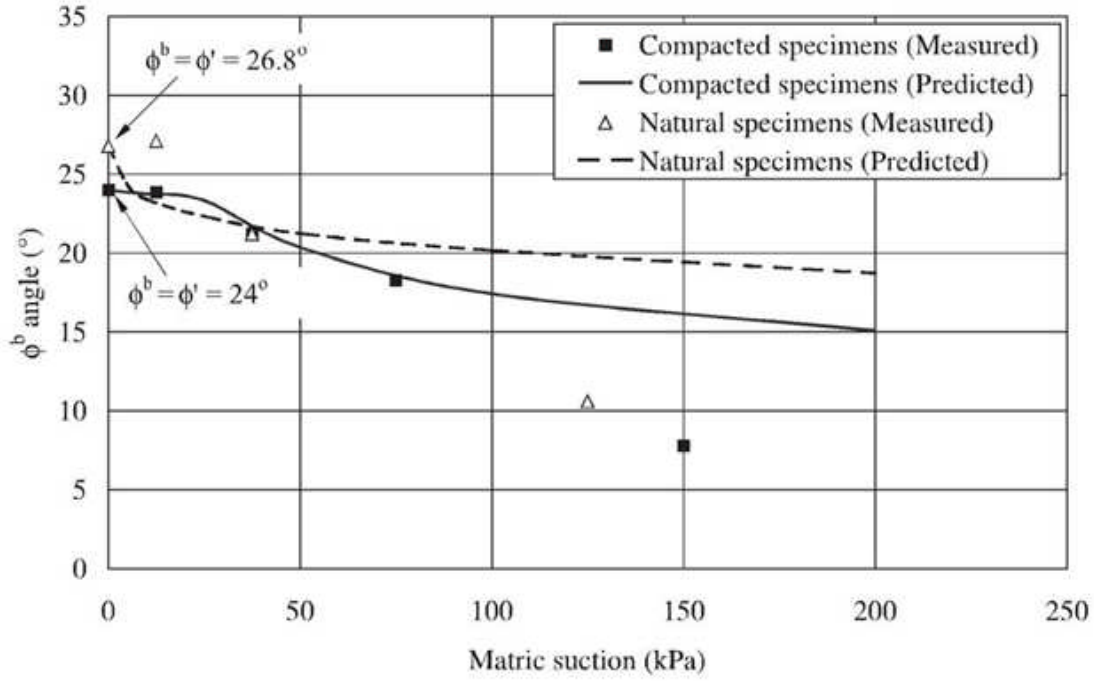

Figure 2-11 Variations of $\varnothing^b$ angles with matric suction for natural and compacted specimens (Zhan and Ng, 2006).

Gebre (2010), under his study on unsaturated expansive clay soils of Addis Ababa, has compared his result with natural specimens from Zhan and Ng (2006) for the contribution of suction to shear strength and the variation of $\emptyset^b$ angle with suction. He found the result of Zhan and Ng (2006) to be higher even though he obtained the trend for the suction to shear strength curve similar at low matric suction.

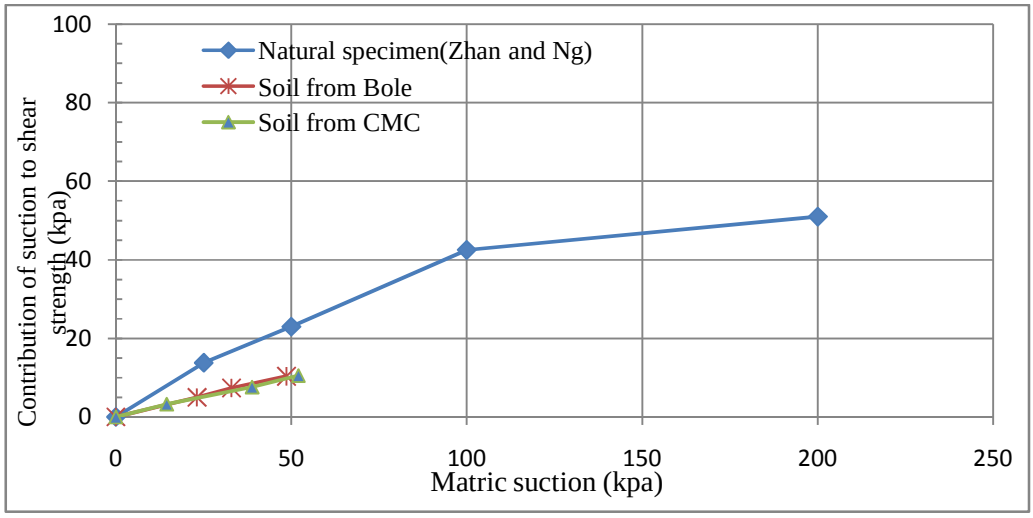

Figure 2-12 Contribution of suction to shear strength for Bole and CMC area soils together with natural specimens of Zhan and Ng (2006).

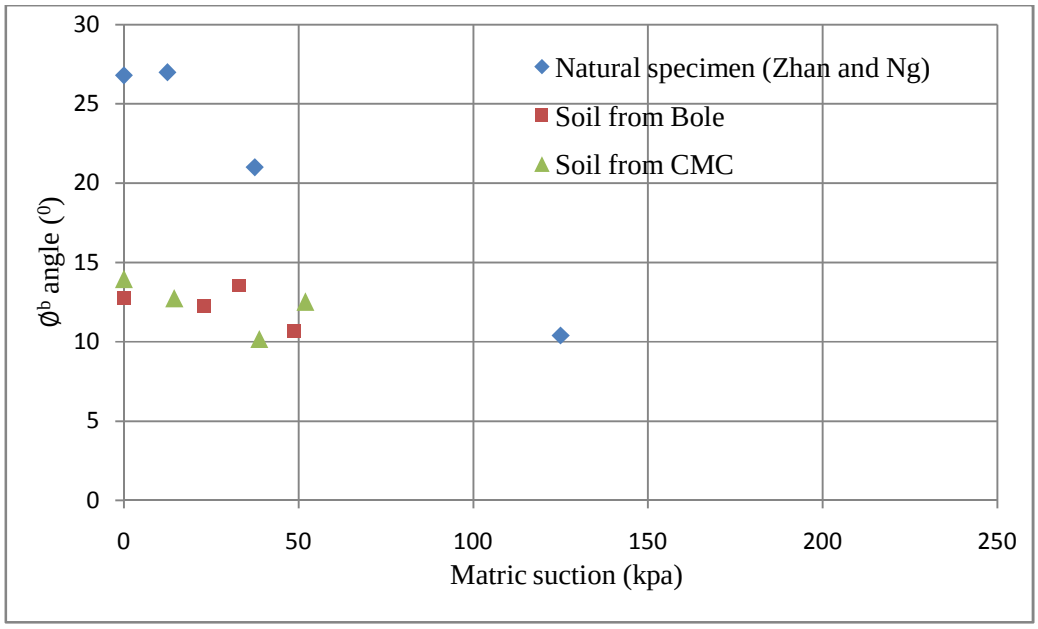

Figure 2-13 Variations of $\emptyset^b$ angles with matric suction for Bole and CMC area soils together with natural specimens of Zhan and Ng (2006).

3. LABORATORY TESTS AND RESULTS

3.1. Index Properties

Index properties are properties of soil which are not of primary interest to geotechnical engineers but which are indicative of the engineering properties. The following index property tests were conducted to understand the physical properties of the soil under consideration.

3.1.1. Grain size analysis test

ASTM Designation D422-63 was followed to carry out wet sieve and hydrometer analysis on disturbed sample and percent finer against size of soil particle in millimeter on a semi-log scale is plotted. From this curve the proportion and type of soil grains are determined. The result of the test is given in Table 3.1.

Table 3-1 Grain size distribution results of the study area (According to BS)

Location	Depth (m)	Gravel (%) (size>2.00mm)	Sand (%) (0.006-2.0mm)	Silt (%) (0.002-.006mm)	Clay (%) (<0.002mm)
AMU –HSC	2.5	2.3	2.9	40.13	54.67
Yetnebersh	2.0	2.0	2.4	31.99	63.63
Muluwengel	2.0	2.7	2.6	46.26	48.44
Edgetber Kebele	2.0	0.7	3.49	39.13	56.77
Doysa Kebele	2.0	0.4	0.9	30.22	68.48
Wubete Hotel	1.5	3.9	8.7	25.46	61.94
Mesgid	1.0	4.7	6.8	39.44	49.06
Woreda Firdbet	1.5	2.0	5.1	34.69	58.21
Shecha highschool	1.5	0.9	4.0	33.65	61.45
Chamo Kebele	1.5	3.5	7.7	29.54	59.26

3.1.2. **Consistency Limits - Atterberg Limit Tests**

The presence of clay mineral in fine-grained soils makes the soil to be remolded without crumbling if some moisture exists. This cohesive nature is caused by the adsorbed water surrounding the particles. At very low moisture, the soil behaves more like solid but when the moisture gets very high, the soil and water may flow like a liquid. Atterberg developed Liquid Limit, Plastic Limit and Shrinkage Limit to describe the consistency (Das, 2002).

The shrinkage limit is much less commonly used than the liquid limit and the plastic limit, but it can be utilized to evaluate the shrinkage potential and possibility of development of cracks in earth works as well as the expansion potential of clayey soils (R. Kerry Rowe, 2001). The plasticity index, PI, is the difference between the liquid limit and the plastic limit. The difference between the liquid limit and the shrinkage limit gives the shrinkage index SI. BS-1377 -2:1990 is followed for the testing procedures and the values gained are presented in Table 3.2.

Table 3-2 Aterberg Limits, Free swell and Specific Gravity results of the study area

Location	Depth (m)	Liquid Limit (%)	Plastic Limit (%)	Plastic index (%)	Volumetric Shrinkage Limit (%)	Shrinkage index (%)	Free Swell (%)	Specific Gravity
AMU –HSC	2.5	120	46	74	12	108	137.0	2.72
Yetnebersh	2.0	107	49	58	12	96	137.5	2.69
Muluwengel	2.0	95	45	49	12	83	94.0	2.70
Edgetber Kebele	2.0	108	46	62	9	99	127.5	2.74
Doysa Kebele	2.0	129	52	77	12	117	165.0	2.63
Wubete Hotel	1.5	98	41	56	17	81	107.5	2.70
Mesgid	1.0	104	51	53	11	93	95	2.66
Woreda Firdbet	1.5	108	47	61	12	96	105	2.74

Shecha highschool	1.5	102	48	55	13	89	147.5	2.80
Chamo Kebele	1.5	102	52	50	12	91	110	2.73

3.1.3. Specific Gravity Test

Specific gravity of soil is the ratio of the unit weight of solids in the soil to the unit weight of water. It is determined using ASTM D 854-83 and the results are given in Table 3.2.

3.1.4. Free Swell Test

A 10 cm^3 (V_i) dry soil passing thorough a No. 40 (425micron) sieve is poured into a 100 cm^3 graduated cylinder filled with water. The volume of settled soil is measured after 24 hours which gives the value of V_f. The ratio of the increase in volume to its initial, $(V_f - V_i)/ V_i$ expressed in %, is taken as the free swell. And the results are indicated in Table 3.2.

3.1.5. Classification of the soil under study

As classification systems provide a common language to concisely express the general characteristic of soils without detailed description, the soil under study is classified according to USCS; AASHTO and Single Index Method as follows:

i) Classification according to USCS

The USCS uses symbols for particular size groups. These symbols and their representations are: G – gravel, S – Sand, M – Silt, C – Clay. These are combined with other symbols expressing gradation characteristics – W for well-graded and P for poorly graded – and plasticity characteristics – H for high and L for low, and a symbol O for the presence of Organic material. The flowchart shown in Figs. 3.1 provides systematic means of classifying an inorganic fine-grained soil according to the USCS (Budhu, 2007). According to this classification scheme, the soil under study is more likely to be CH as the clay fraction is higher than the silt fraction and as higher plasticity is observed having more that 50% of particles with a grain size less than 0.075mm.

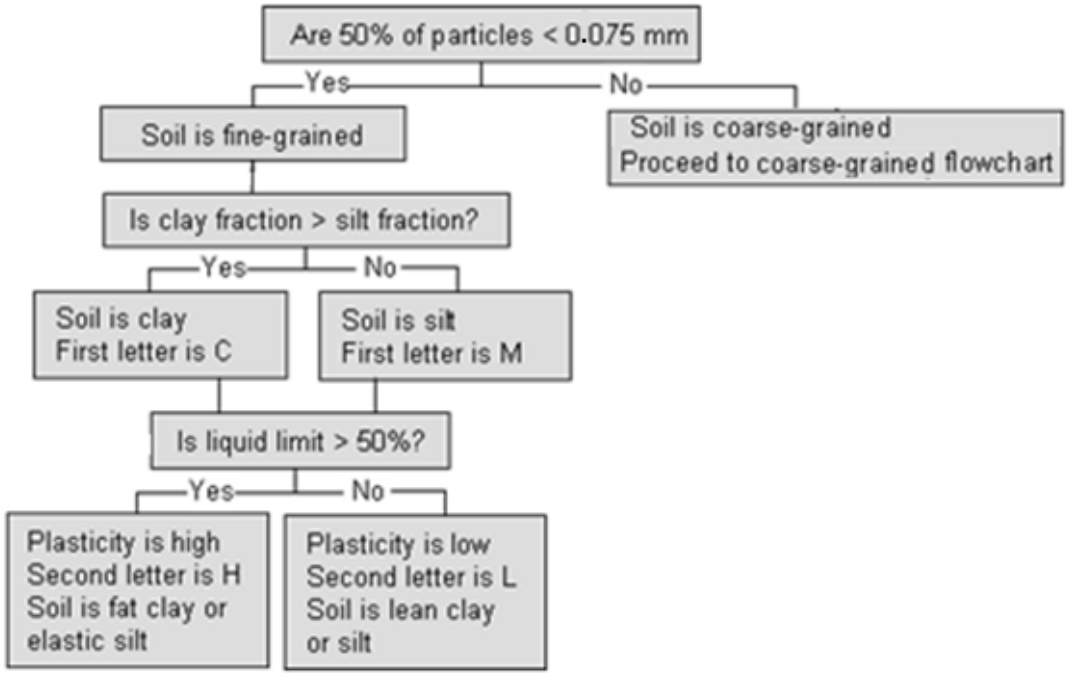

Figure 3-1 Unified soil classification flowchart for inorganic fine-grained soils (Budhu,2007)

Experimental results from soils tested from different parts of the world were plotted on a graph of plasticity index (ordinate) versus liquid limit (abscissa). It was found that clays, silts, and organic soils lie in distinct regions of the graph – the plasticity chart, Figure 3.1. The A-line separates clays from silts and the U-line indicates the upper limit of the relationship between PI and LL. Accordingly, the soil under study is plotted on the plasticity chart. The soils from AMU-HSC and that around Wubete Hotel touch the A-line with the rest falling near below it – directing to the silt region. Thus, the plasticity chart may not be fully applicable for the soil under study. However, this may need further investigation as the laboratory results of Atterberg limit tests and free swell tests reflect that the soil contains a significant amount of clay.

ii) Classification according to AASHTO

According to this system, soil is classified into seven major groups: A-1 through A-7. Soils classified under groups *A-1*, *A-2*, and *A-3* are granular materials of which 35% or less of the particles pass through the No. 200 (0.075mm) sieve. Soils of which more than 35% pass through the No. 200 (0.075mm) sieve are classified under groups *A-4*, *A-5*, *A-6* and *A-7*. These soils are mostly silt and clay-type materials. According to this system the soil of the study area falls in the

region of *A-2-7* and *A-7-5* (Figure 3.2).This means the soil under interest is plastic clay which has a high volume change capacity between wet and dry states.

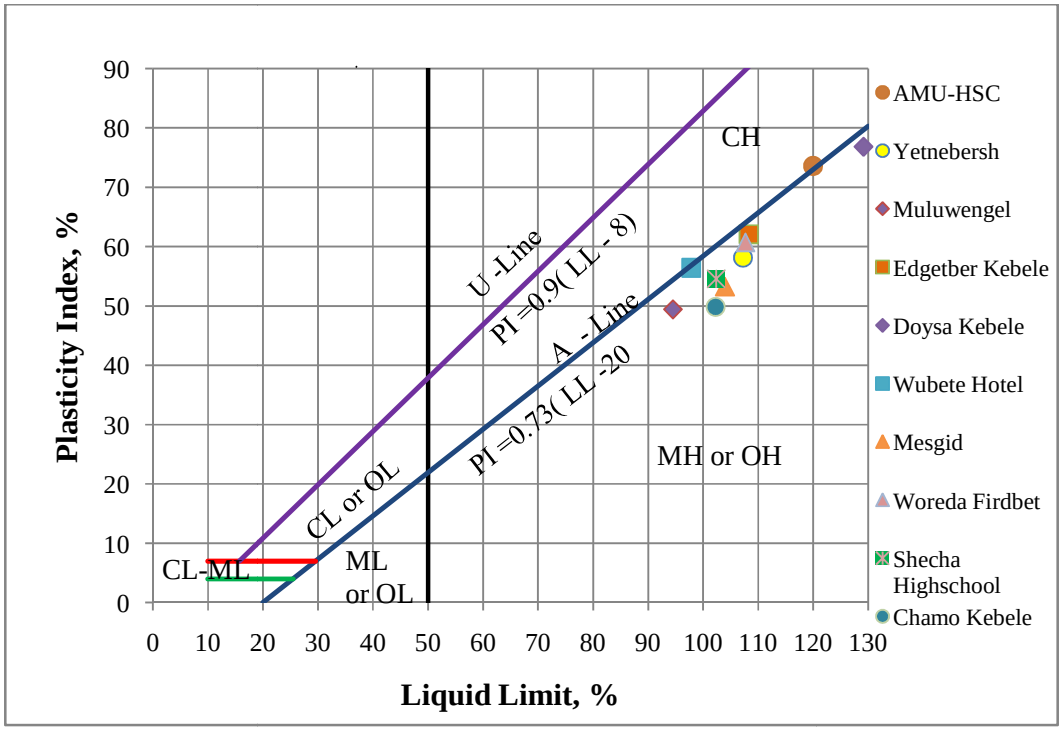

Figure 3-2 Plasticity chart of the study area according to USCS

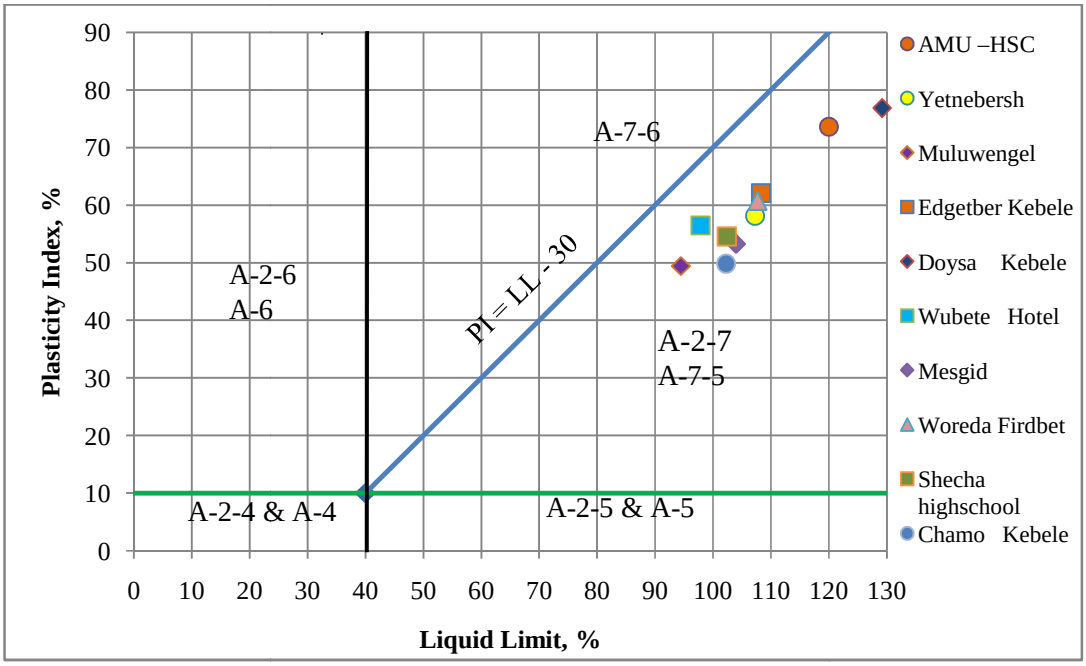

Figure 3-3 Plasticity chart of the study area according to AASHTO

i) Classification according to Single Index Method

According to Seed, Woodward and Lundgreen (in Chen, 1988), Plasticity Index is a parameter which can be used as a preliminary indicator of the swelling characteristics of a soil. But it should be noted here that high index property doesn't necessarily mean high swelling potential while the converse may be true. The following values are proposed to relate swelling potential with index property.

Table 3-3 Expansive soil classification based on plasticity index (Chen, 1988)

Swelling potential	Plastic index
low	0 - 15
medium	10 - 35
High	20 - 55
Very high	35 and above

Relating the Plasticity Index of the soil of the study area with the above given range reveals that the soil falls in the range of very high swelling potential.

Shrinkage Limit is also used as a guide to the determination of potential expansiveness. Altmayer (Chen, 1988) suggested the following relation.

Table 3-4 Expansive soil classification based on Shrinkage limit(Chen, 1988).

Shrinkage Limit, %	Degree of expansion
< 10	Critical
10 - 12	Marginal
>12	Non critical

This method indicates the soils at the Edgetber kebele exhibit critical degree of expansion, those around Wubete Hotel, Woreda Firdbet, Shecha Highschool and Chamo kebele on a marginal state and the rest being non critical.

3.2. Swelling Pressure Test

According to Method A (Swell-Consolidation test) of ASTM D 4546-96, the seating pressure of 7 kPa was applied to the clay specimen. After the initial deformations at the seating pressure

were complete, the specimen was inundated with water in the oedometer cell and allowed to swell vertically. After the sample had swollen to its maximum extent, the specimen was loaded until it regains its initial volume and the pressure required to do this is designated as Swelling Pressure. The results from this test are shown in Table 3.5. Sample calculations are detailed in Appendix A.

Chen, (1988) indicated that the initial density of the soil, whether for undisturbed or remolded sample, to be the only element that affects the swelling pressure. For undisturbed soil, dry density is the in situ characteristics and the swelling pressure at this state can be used to directly describe the swelling characteristics. The in situ dry density can be calculated from the relation:

$$\gamma_{bulk} = \frac{weight\ of\ \ wet\ soil\ in\ the\ ring}{volume\ of\ \ the\ ring}$$

$$\gamma_{dry} = \frac{\gamma_{bulk}}{(1+\omega)}$$

where, ω is the natural moisture content.

Table 3-5 Swelling Pressure Test results of the study area

Location	Depth of Sampling (m)	Natural moisture content (%)	In situ dry density, γ_d (gm/cc)	Swelling Pressure (kPa)
AMU –HSC*	2.5	29.03	1.23	265.17
Yetnebersh	2.0	33.65	1.31	571.29
Muluwengel	2.0	32.50	1.28	246.60
Edgetber Kebele	2.0	31.76	1.30	494.77
Doysa Kebele	2.0	26.82	1.29	464.90
Wubete Hotel	1.5	32.69	1.23	250.15
Mesgid	1.0	39.19	1.18	74.53

Woreda Firdbet	1.5	35.77	1.26	481.77
Shecha highschool	1.5	40.78	1.22	458.28
Chamo Kebele	1.5	39.15	1.20	224.37

*Sample was allowed to air-dry prior to testing for it has revealed no swelling.

Teklu (2004) has obtained the sweeling pressure of black expansive soils of Addis Ababa varying between 57 and 420 kPa. According to Nigussie (2004), the swelling pressure of expansive soils from Bahir Dar has a value ranging between 75.95 and 547.52kPa. This indicates the measured swelling pressures are not as such out of range. However, when observing the value obtained for Wubete hotel and Shecha highschool area pits, for approximately the same in situ dry density and percent clay particles, a big difference is seen on the measured swelling pressure. This might be due to the difference for the active clay mineral amount, which could have been verified by mineralogical test that was not done as part of this study.

3.3. Shear Strength Tests

The drainage conditions of the sample is generally the deciding factor in choosing a particular type of the test in the laboratory since the test specimen should conform as closely as possible to the conditions under which the soil will be stressed in the field. Saturated soils of clays, very fine sand, silts and silty sands are likely to fail in the field under condition similar to those under which consolidated quick (CU) tests are made due to their poor drainage qualities (Murthy, 2007). The long time duration required with unsaturated soil testing and the very low permeability of expansive clay have forced the investigator to conduct Consolidated Undrained test.

3.3.1. Testing Apparatus

Electronically controlled, both the conventional and modified triaxial, testing equipments were used for this study. The conventional triaxial equipment, Figure B-3 in Appendix B, was used for the saturated case and a 50kN modified double wall triaxil machine, Figure 3.4, manufactured in England by Wykeham Farrance was utilized for unsaturated testing. The provision of a specially designed high-air entry disk and the means for independent measurement

of pore air and pore water pressures in unsaturated testing machine helps the use of axis-translation for the desired matric suction application.

Figure 3-4 Modified triaxial apparatus

The pore air pressure is usually controlled through a coarse corundum disk placed on top of the soil sample and the pore water pressure is controlled through a saturated high air entry ceramic disk sealed to the pedestal, with the help of pore air and pore water pressure measuring transducers respectively. The equipment is also fitted with volume measuring units for the measurement of the amount of water entering and out of the sample, and load cell for measuring the amount of axial load. Each of the measuring unit is connected to the 16-channel data logger calibrated for specific measurements of interest and in turn connected to PC where the appropriate software has been installed.

3.3.2. Sample Preparation

Undisturbed soil samples were collected from the field in 100 mm diameter sampling tubes from a test pit dug to a depth of 2.5m (Figure B-1 a). The sample in the sampling tube was wrapped as much as possible placing a sufficient wax, rag and covered by clinging plastic in order to

eliminate any moisture loss from it until the soil is used for testing (Figure B-1 b). From this tube, the test specimen having dimension of 70mm dia. by 140mm height was prepared for unsaturated test and specimen with diameter of 38mm and 75mm height was taken for saturated testing.

To take out the required dimension of soil sample for unsaturated case, the sample extractor having internal dimension of 70mm dia. with 140mm height has been pushed in to the large size sampling tube (the aforementioned 100 dia. tube) with which the sample has been brought from the field. After the sampling tube (70mm x 140mm) is pushed into the larger size tube, the soil with the sampler tube has been taken out and finally the soil sample with the required dimension is extruded from the sampler tube with another sample extractor. The specimen for the saturated condition is also cautiously trimmed from the extractor specified for it.

Once the sample is prepared and made ready for testing, it is mounted on the base pedestal of the machine which is properly flushed by letting freshly de-aired water to pass continuously in the system to avoid any entrapped air. This is done by opening one at a time the volume change units, pressure bladders, back and cell pressure line taps so that virtually no more air bubbles can be seen coming out of the system. Doing this, the flushing process saturates the high air entry disk when the back pressure line is open and kept for a long time.

The sample is then placed on a pre-saturated high air entry disk and covered with a rubber membrane and now fixed with bottom O-rings. Next, the course porous stone and the top loading cap are positioned on top of the specimen. After placing O-rings on the rubber membrane surrounding the top cap, the cell chamber is put in its proper place and filled with de-aired water. The cross-sectional view of the apparatus with the sample mounted looks like the one shown in Figure 2.8 (a). The mounting of samples on the conventional triaxial machine follows the same procedure except, placing saturated porous stone on the base instead of the high air entry disk.

3.3.3. Testing procedure

3.3.3.1. **Saturation Stage**

Initially, unsaturated samples either undisturbed or compacted must be saturated prior to testing (Fredlund and Radigho, 1993). The objective of the saturation stage is to ensure that all the voids are filled with water without producing undesirable prestressing of the specimen or allowing the soil to swell. This is often achieved by raising the pore pressure in the specimen to a level high enough for the water to absorb into solution all the air originally in the voids. There are two methods of saturating a sample: a) applying compression under undrained condition; or b) back-pressuring de-aired water into the soil specimen (BS – 1377-8: 1990). Saturation by compression the specimen is not as efficient as applying a backpressure to the water phase (Fredlund and Radigho, 1993). The saturation of the soil specimen in series of tests was accomplished by using the backpressure technique. Here it becomes worthy to mention that during saturation process of expansive soil, the soil gets a considerable volume change that raises difficulty in measuring the dimensions of the soils at the start of consolidation. Fortunately, as the test specimens for this study have already swollen at the site (see Table 3.5) this problem was minimal.

BACKPRESSURE TECHNIQUE

The predetermined cell pressure and backpressure were applied at several stages keeping the difference between the two values to 10 kPa until saturation is achieved. The cell pressure should always be larger than the backpressure, so that the effective stress is positive. Saturation of the sample is ensured when the pore water pressure increment divided by the backpressure increment parameter *B* which is given by a relation

$$B = \frac{\delta u}{\delta \sigma}$$

(Where δu-change in pore water and $\delta \sigma$-change in stress) is equal to or greater than 0.95 (BS-1377-8:1990).

3.3.3.2. **Consolidation stage**

The objective of the consolidation stage is to bring the specimen to the state of effective stress and matric suction required for carrying out the compression test. It follows immediately after the saturation stage. Consolidation of the specimen for these tests is isotropic. To start this stage,

the back pressure valve remains closed and the final pore water pressure and volume-change readings are recorded at the end of the saturation stage. The effective stress in the specimen is increased to a desired value by raising the cell pressure *(σ_3)* in the cell pressure line and adjusting the back pressure if necessary.

The pore air pressure is controlled to the value which is the sum of the required matric suction and the pore water pressure at the end of the saturation stage by opening the pore air line. Now record the pore pressure when a steady value *(u_i)* (in kPa) is reached and take the reading of the volume-change indicator. At a convenient moment, start the consolidation stage by opening the back pressure valve and record the readings of the volume-change indicator at suitable intervals of time until there is no further significant volume change. When consolidation is complete, record the reading of the volume-change indicator, and calculate the total change in volume *(ΔVc)* during the consolidation stage. Record the pore pressure u_c (in kPa) and proceed to the compression stage.

3.3.3.3. **Shearing stage**

After the consolidation stage, the samples were axially loaded in compression keeping the cell pressure constant and closing drainage valves so that the test will be undrained. The cell loading piston is adjusted just to touch the top of loading cap. All the tests were performed under a strain-controlled condition applying a constant rate of displacement 0.076mm/min which is calculated based on the procedure in BS-1377-8:1990. The sample is then sheared by pressing the switches of the compression frame motor, logger, and computer ensuring that the drainage valves are closed. The changes in displacement, pore water pressure, pore air pressure and the load are measured automatically.

The test is stopped when one of the following criteria has been clearly identified. The different failure criteria produce similar shear strength parameters (Fredulnd and Radighoo, 1993).

a) Maximum deviator stress;

b) Maximum effective principal stress ratio;

c) Constant shear stress and constant pore pressure.

3.3.4. Results obtained from Consolidated Undrained Test

The laboratory testing program was planned and carried out in two main groups in order to fulfill the objective of the study. The first testing group deals with saturated samples (i.e., samples with zero matric suction) aiming to evaluate the effective shear strength parameters, *c'* and ϕ' as well to compare the behavior of saturated samples with that of unsaturated ones. The second group is all about the unsaturated samples. The values of the initial matric suction and other specifications are tabulated in Table 3.6.

The conventional triaxial shear tests at zero matric suction were carried out on saturated or nearly saturated natural specimens. Figure 3.5 shows the deviator stress vs. axial strain curve and Figure 3.7 plots the Mohr-Coulomb failure envelops obtained from these tests. Figure 3.6 depicts the deviator stress vs. axial strain curve obtained from the tests with the modified triaxial equipment for a constant net confining pressure and increasing matric suction applications.

Table 3-6 Test parameters used for consolidated undrained test (for unsaturated and saturated soil case)

Test pit	Sample Number	Effective Consolidation Pressure (kPa)	Initial Matric suction, h_m (kPa)
AMU-HSC site	S-1	200	0
	S-2	250	0
	S-3	300	0
	S-4	200	100
	S-5	200	150
	S-6	200	200

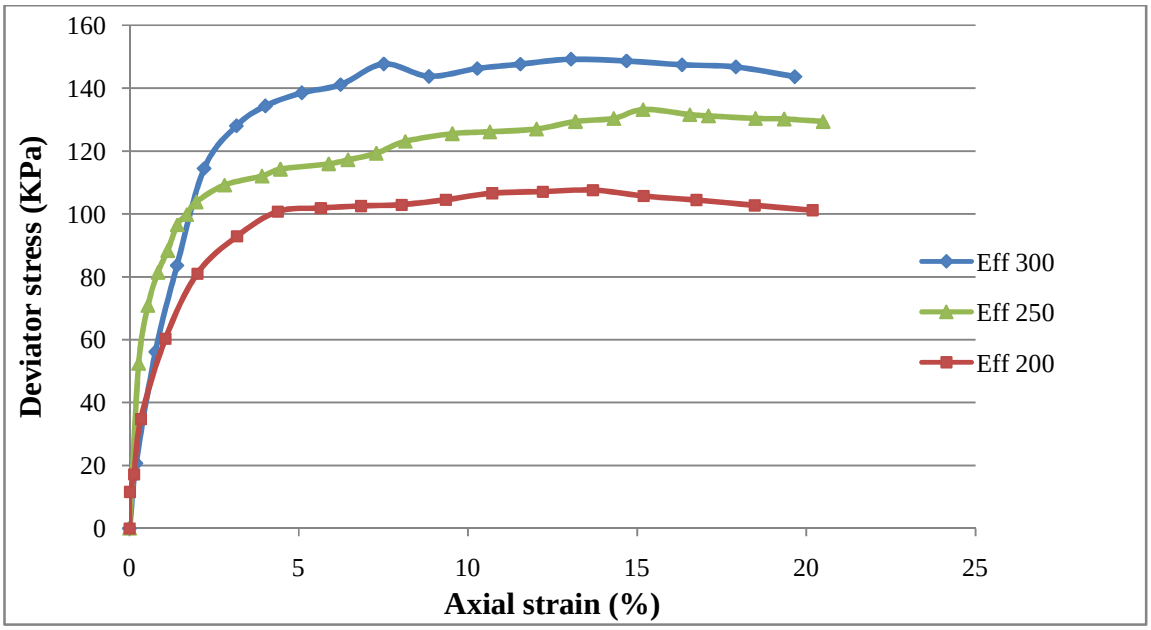

Figure 3-5 Deviator stress Vs Axial Strain for saturated soil under the effective consolidation stresses of 200 kPa, 250 kPa and 300 kPa.

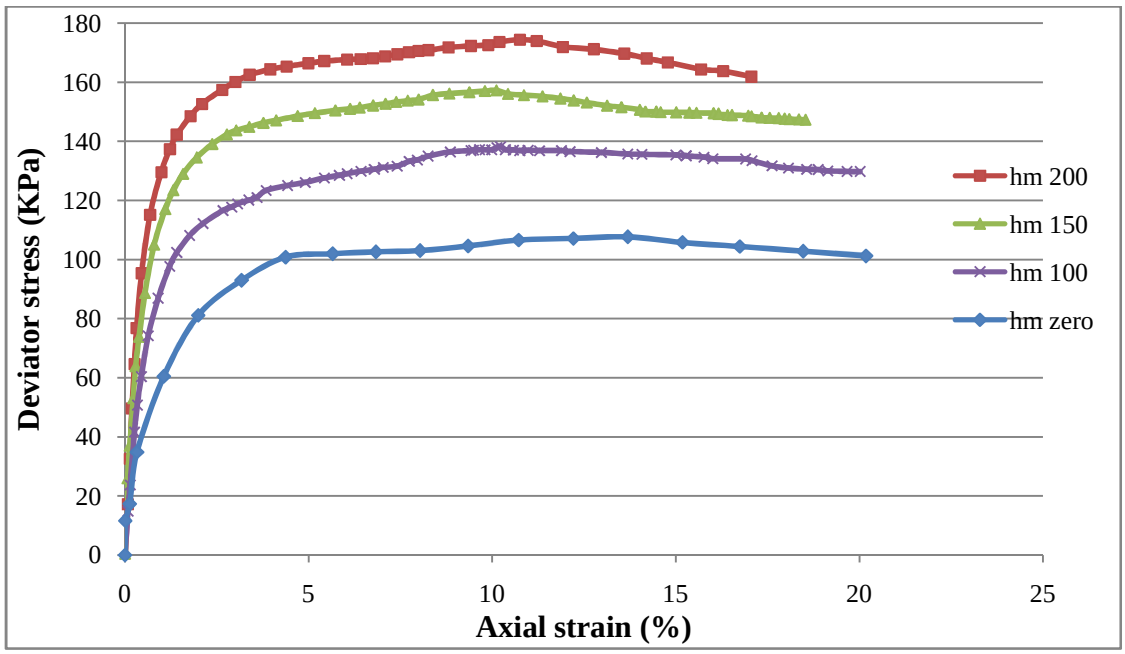

Figure 3-6 Deviator stress Vs Axial Strain for effective consolidation stress of 200 kPa varying matric suction.

For the analysis of the $\varnothing^b$ parameter, which is a function of matric suction of the soil, the following procedures have been followed.

1. Mohr circle for the net normal stress has been drawn for maximum deviator stress obtained from triaxial test carried out on saturated soil sample. Then, a best tangent line for the three circles has been drawn to obtain the *c'* and $\varnothing$' values of the soil.
2. Mohr circle under the effect of the same net confining pressure, at various matric suctions is drawn for the maximum deviator stress.
3. By drawing a tangent line parallel to the one obtained for saturated soil to the Mohr circles drawn for unsaturated case, the value of cohesion where the failure line intersects the shear stress axis has been taken.
4. Plotting the values of shear stress obtained from step 3, on the graph shear stress versus matric suction axis, the value of $\varnothing^b$ is obtained from the best fitting line.

The parameters, which are used to draw Figures 3.7 and 3.8, are tabulated in Table A-9 and Table A-10 in appendix A and the results obtained from the Figures are summarized in Table 3.8.

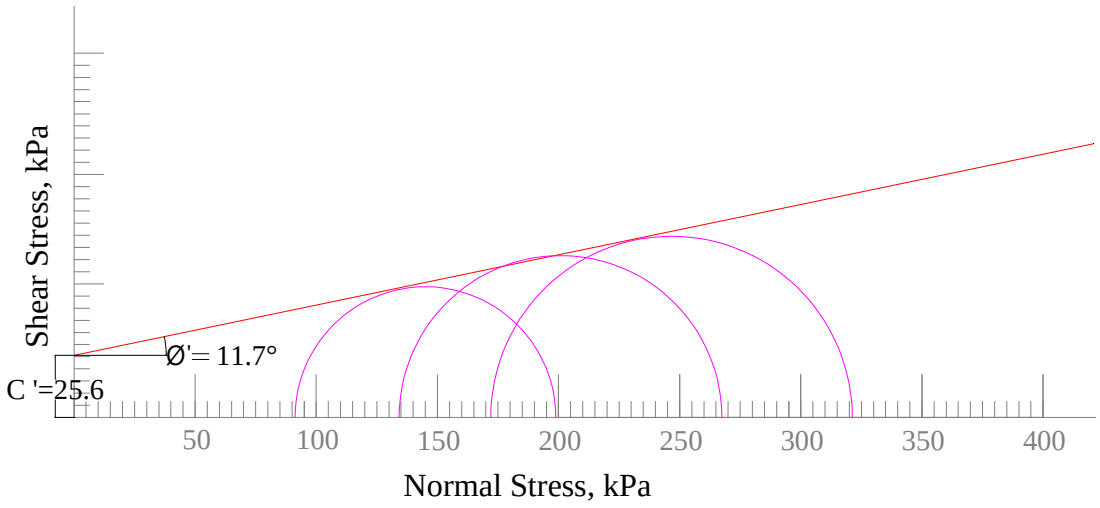

Figure 3-7 Mohr circle for saturated soil under the effect of ($\sigma_{3\,(1)}$ = 200, $\sigma_{3\,(2)}$ =250 and $\sigma_{3\,(3)}$ =300 kPa) effective consolidation pressure.

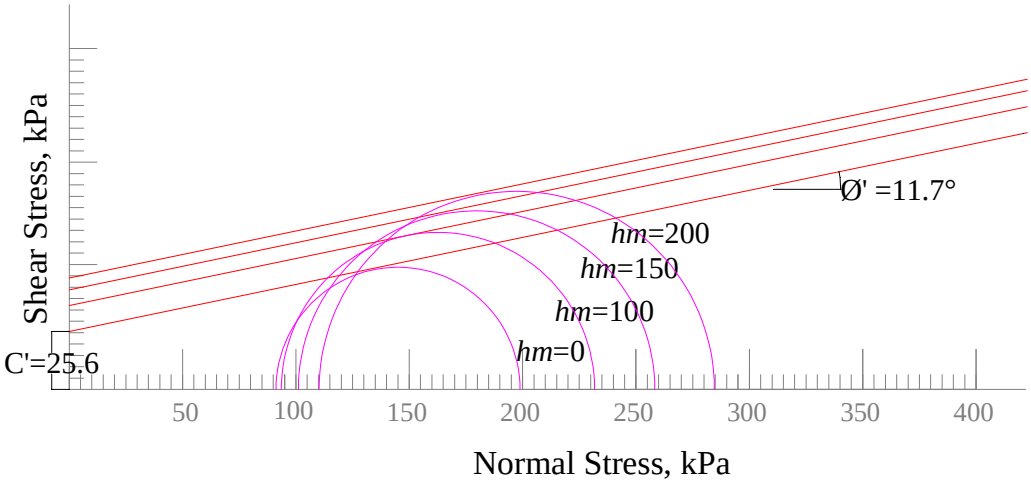

(a)

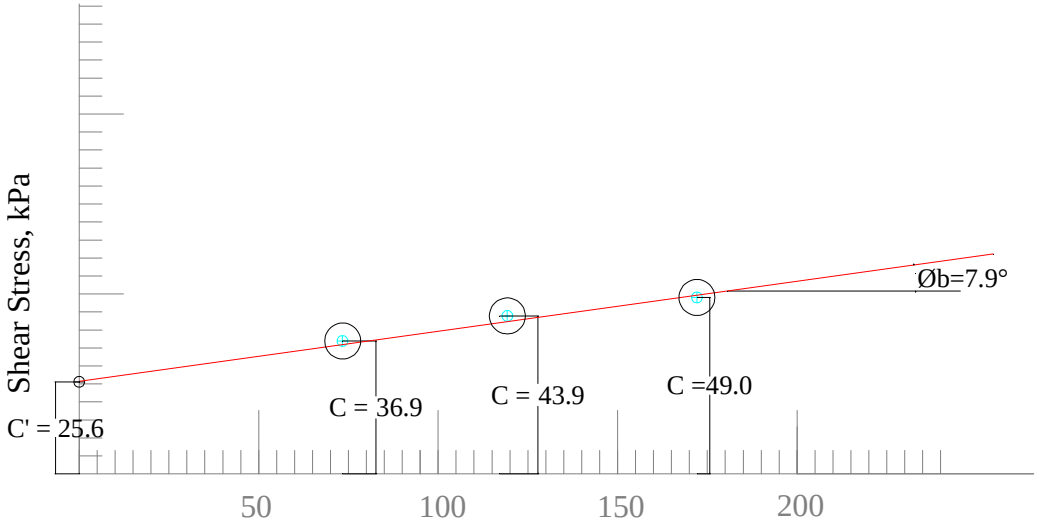

(b)

Figure 3-8 Two-dimensional presentation of failure envelope (a) failure envelope projected on the shear stress versus net normal stress plane, (b) intersection line between the failure envelope and the shear stress versus matric suction plane.

Table 3-7 Summary of the results obtained for the shear strength parameters.

Test pit	Sample no.	Effective consolidation pressure(kPa)	C' (kPa) (for h_m=0)	C (kPa)	Matric suction, h_m (kPa)	$\emptyset'$(deg.) (for h_m =0)	$\emptyset^b$(deg.)
AMU-HSC Site	S-4	200	25.6	36.9	73.34	11.7	8.8
	S-5	200		43.9	119.28		8.6
	S-6	200		49.1	176.46		7.2

To express the unsaturated shear strength of the town in detail, extra tests would have been performed taking additional test pits but because of long repetitive power interruption for about 6 month and/or more, this became unattainable to go further within the available period. It is not as such easy to express in words how difficult it was to lose each 15 to 16 days in response to wastage of undisturbed samples due to pressure release whilst the electric power went off in the consolidation and shearing stages.

4. DISCUSSIONS OF TEST RESULTS

4.1. Validation of Previously Developed Swell Prediction Equations for the Soil Under Study

Since the laboratory-swelling test is a difficult and an expensive process for practicing engineers and small builders, empirical methods that make use of the swelling potential, as determined from index and/or physical properties such as liquid limit, have increasing popularity. Obviously, the proposed equations might have served their purpose in the place where they have been specifically developed. Nonetheless, it is worthwhile to test these suggested equations on soils of the study area and to evaluate the outcome. The comparisons are given in Table 4.1.

Table 4-1 Comparison of previously developed equations with measured values

Location	Depth of Sampling (m)	Measured Swelling Pressure (kPa)	Proposed Eqn. by Dagmawe Nigussie (kPa)	Proposed Eqn. by Daniel Teklu (kPa)		Proposed Eqn. by Vijayvergiya and Ghazzaly (kPa)	Proposed Eqn. by Nayak and Christensen (kPa)	Proposed Eqn. by Komornik and David (kPa)
AMU–HSC	2.5	265.17	329.35	250.26	140.77	679.92	134.32	247.01
Yetnebersh	2.0	571.29	259.61	650.76	701.38	460.87	109.59	113.88
Muluwengel	2.0	246.60	288.58	408.25	322.74	138.85	68.84	63.42
Edgetber Kebele	2.0	494.77	257.80	586.95	543.63	464.05	106.38	132.58
Doysa Kebele	2.0	464.90	437.18	571.78	406.40	2143.94	235.77	482.42
Wubete Hotel	1.5	250.15	411.49	220.42	138.29	124.30	107.19	68.19
Mesgid	1.0	74.53	202.04	109.54	76.18	137.74	58.62	56.67
Woreda Firdbet	1.5	481.77	216.00	339.59	318.41	329.99	90.81	94.52
Shecha highschool	1.5	458.28	188.62	189.47	185.27	163.60	75.06	50.57

Chamo Kebele	1.5	224.37	261.64	139.50	106.21	139.77	70.63	53.92

As can be observed from the above table, none of the equations predict well the swelling pressure for the soil under consideration. This could mainly be due to variation of the nature of the soil, environmental, climatic condition and geologic formation of the region where the relation is developed to the study area.

4.2. Development of New Predictive Model

In order to take into account the combined effects of the soil properties on swelling parameters and to obtain predictive equations with higher coefficients of correlation than those obtained from simple regression, multiple regression analyses were carried out using SPSS16.0 computer software. Out of these, equations with higher correlation coefficient were selected and using these equations the swelling behavior of the soil of the study area were calculated. Then a graph is plotted which shows the measured value against the predicted or calculated value. Finally 5 equations, listed below, are selected which predicted the measured value better than the others. A typical regression output file of the software has also been presented.

$Log\ S_p = -3.059 + 0.003PI + 4.28\gamma_d$, where γ_d in g/cm3; PI in %, R^2=0.578 (4.1)

$Log\ S_p = -6.744 + 0.029\omega_i + 0.009LL + 5.826\gamma_d$, where γ_d in g/cm^3, ω_i= natural moisture content, R^2=0.754 (4.2)

$Log\ S_p = -3.122 - 0.002SI + 0.004\gamma_d + 0.02C$, where γ_d in kg/m^3; C = clay fraction finer than 0.002mm in %, R^2=0.652 (4.3)

$Log\ S_p = -7.908 + 0.058\omega_i - 0.019LL + 0.042PI + 6.394\gamma_d$, where γ_d in g/cm^3, ω_i, LL & PI in %, R^2=0.891 (4.4)

$Log\ S_p = -3.831 + 0.007\omega_i - 0.0212A_c + 0.005\gamma_d$, where γ_d in Kg/m^3; $A_c = \frac{PI}{C}$, R^2=0.593 (4.5)

Regression analysis for equation 4.2

Variables Entered/Removed[b]

Model	Variables Entered	Variables Removed	Method
1	densityingcm3, LL, w[a]	.	Enter

a. All requested variables entered.

b. Dependent Variable: logSP

Model Summary

Model	R	R Square	Adjusted R Square	Std. Error of the Estimate
1	.823[a]	.677	.516	.18464

a. Predictors: (Constant), densityingcm3, LL, w

ANOVA[b]

Model		Sum of Squares	df	Mean Square	F	Sig.
1	Regression	.430	3	.143	4.201	.064[a]
	Residual	.205	6	.034		
	Total	.634	9			

a. Predictors: (Constant), densityingcm3, LL, w

b. Dependent Variable: logSP

Coefficients[a]

Model		Unstandardized Coefficients		Standardized Coefficients	t	Sig.	Correlations		
		B	Std. Error	Beta			Zero-order	Partial	Part
1	(Constant)	-6.744	3.176		-2.124	.078			
	w	.029	.022	.497	1.318	.236	-.334	.474	.306
	LL	.009	.008	.349	1.143	.297	.298	.423	.265
	densityingcm3	5.826	1.816	.976	3.208	.018	.758	.795	.744

a. Dependent Variable: logSP

4.3. **Assessment of Currently Developed Swell Prediction Models**

The above newly developed models (eqn. 4.1 – 4.5) are used to calculate the swelling pressure of the study area. Then, the results from the current relations are tested to see how well the developed equations have predicted the swelling pressure.

Table 4-2 Values of measured and predicted swelling pressure

		Predicted by the new models				
Site	Sp^1	Eqn. 4.1	Eqn. 4.2	Eqn. 4.3	Eqn. 4.4	Eqn. 4.5
AMU–HSC	265.17	266.83	220.72	474.26	283.13	172.49
Yetnebersh	571.29	527.53	674.78	1581.69	667.41	576.43
Muluwengel	246.6	369.56	320.83	633.37	276.62	380.34
Edgetber Kebele	494.77	491.18	531.54	1034.71	625.09	456.55
Doysa Kebele	464.9	492.75	515.37	1489.70	464.56	370.64
Wubete Hotel	250.15	236.98	178.13	748.20	231.09	226.28
Mesgid	74.53	141.64	159.66	247.38	148.20	129.77
Woreda Firdbet	481.77	328.09	401.23	777.79	533.90	314.93
Shecha highschool	458.28	211.99	293.72	643.78	402.03	232.38
Chamo Kebele	224.37	168.47	200.90	481.17	153.34	183.97

Sp^1 - is measured swelling pressure in the laboratory

The following graphs are plotted to investigate the approximation accuracy of the newly developed formulas. The measured and calculated values are plotted (Figure 4.1 to Figure 4.5) and trend lines are drawn to observe the gap between the measured and the calculated values.

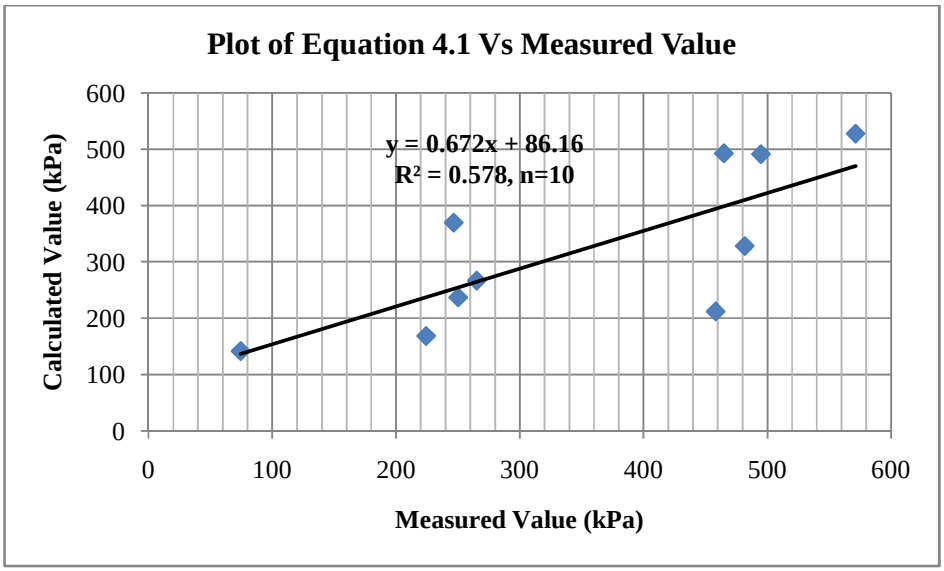

Figure 4-1 The relationships between the measured and predicted swelling pressure for eqn.4.1. The simple coefficient of correlation = 0.76

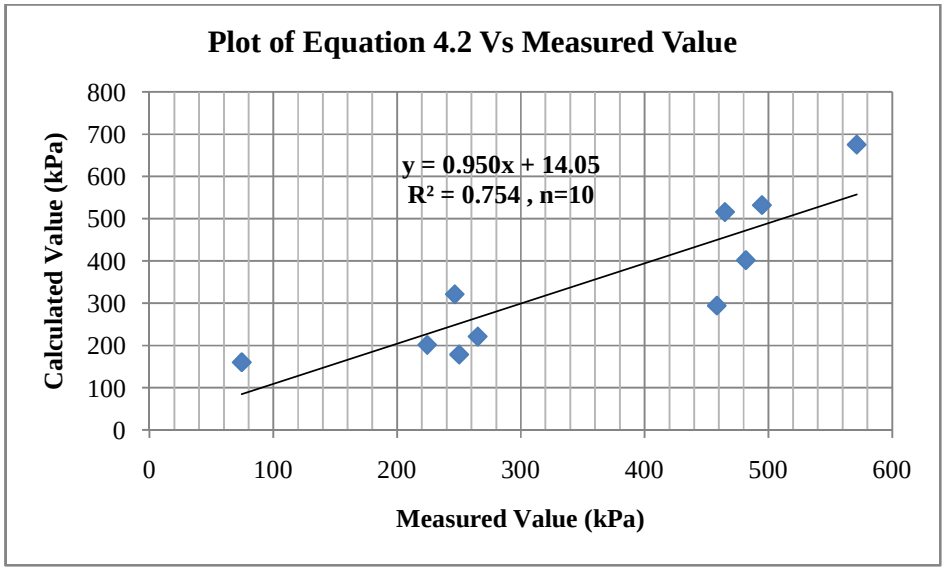

Figure 4-2 The relationships between the measured and predicted swelling pressure for eqn.4.2. The simple coefficient of correlation = 0.87

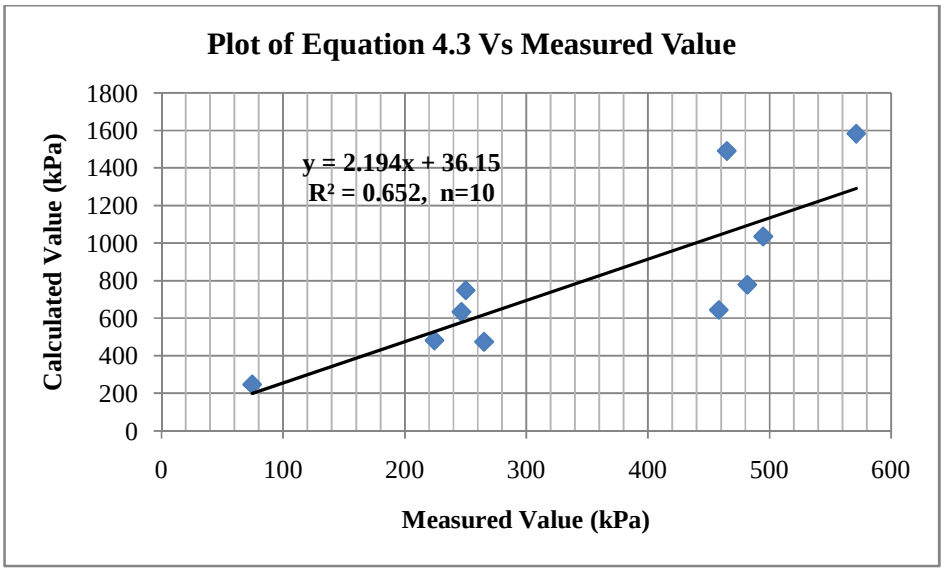

Figure 4-3 The relationships between the measured and predicted swelling pressure for eqn.4.3. The simple coefficient of correlation = 0.81

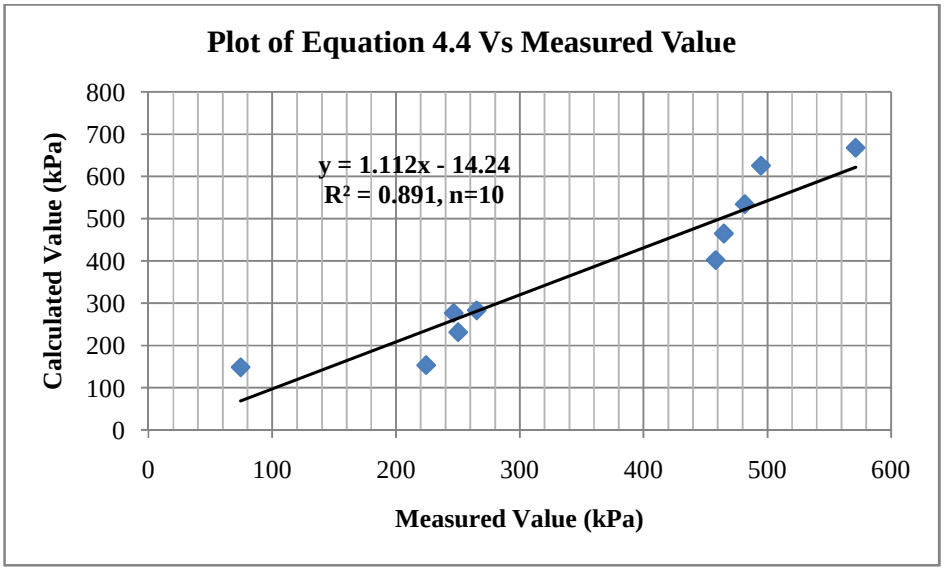

Figure 4-4 The relationships between the measured and predicted swelling pressure for eqn.4.4. The simple coefficient of correlation = 0.94

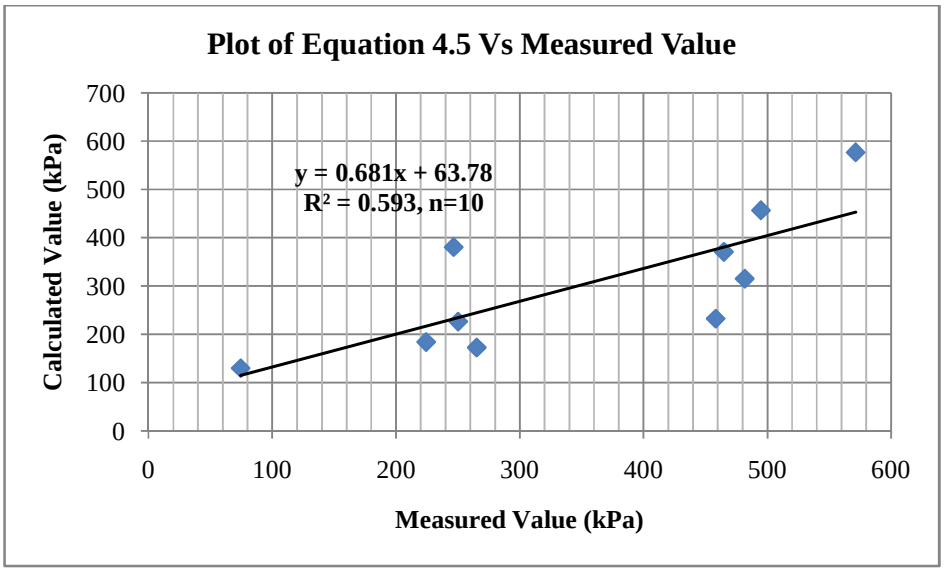

Figure 4-5 The relationships between the measured and predicted swelling pressure for eqn.4.5. The simple coefficient of correlation = 0.77

Observing Figure 4.1 – 4.5, equations 4.2, 4.3 and 4.4 have given a better estimate of the measured swelling pressure with a coefficient of determination of 0.75, 0.65 and 0.89 respectively. Among the three equations, the relation described by equation 4.4 better closes to the measured swelling pressure with about 6 per cent unexpected uncertainty based on the simple coefficient of correlation.

4.4. **Discussion on Triaxial Test Results**

Figure 3.5 points out the increase in shear strength of the soil due to an increase in initial effective confining pressure for the soil under saturated condition. Nevertheless, for the same effective confining pressure, the stress strain diagram of unsaturated specimen is observed to be higher than that of saturated soil sample whilst its basic shape being maintained for strains before failure. On the other hand, for higher matric suctions, under the application of deviator stress, the sample attains some brittle nature so that the stress-strain diagram falls relatively rapid after the maximum deviator stress (Figure 3.6). What is more, from both deviator stress versus axial strain diagram (Figure 3.6) and Table 4.3, the values of the deviator stress increase when the matric suction of the soil increases. This is because as air enters the pores, a contractile skin begins to form around the points of contact between the particles. The capillary action arising from the

suction around the contractile skin increases the normal forces at the inter-particle contacts. This additional normal force will enhance the friction and cohesion at the inter-particle contacts. As a result, the unsaturated soil exhibits more strength than that of saturated soil. It was expected to be so (Fredlund and Radigho, 1993; Zhan and Ng, 2006; Gebre, 2010; W/Medhin, 2010).

Table 4-3 Comparison of failure deviator stress for saturated and unsaturated case

Test pit	Sample state before shear commencement	Effective consolidation pressure(kPa)	Deviator Failure stress(kPa)
AMU-HSC site	Saturated soil sample	200	107.61
	Matric suction 100 kPa		138.24
	Matric suction 150 kPa		157.22
	Matric suction 200 kPa		174.35

The failure envelope for saturated soils is represented on two-dimensional plots (Figure 3.6). But the shear strength of unsaturated soils are dependent on the two stress state parameters (i.e. the normal stress and the matric suction axis) as a result of this the failure envelope has been drawn on three dimensional plots, see Figure 4.6.

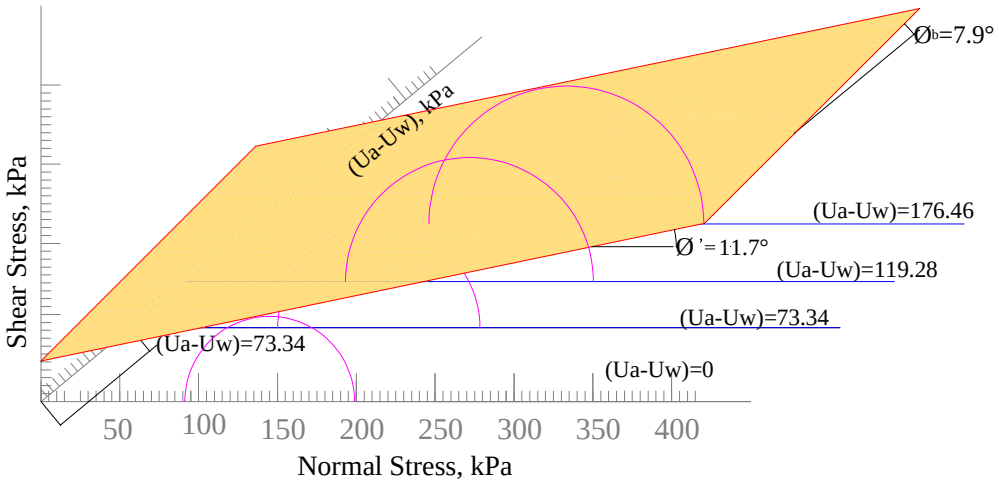

Figure 4-6 Failure envelopes for unsaturated soil from AMU-HSC area.

The soil under the study is also compared with the results obtained from Gebre(2010), and Zhan and Ng (2006) for China soil. From Figure 4.7 and Figure 4.8, it can be noticed that the result of comparison by Gebre (2010) shows similar suction to shear strength curve both being higher

than the soil under study for low matric suction. Figure 4.7 shows contribution of matric suction to shear strength of the soil samples. The data points were obtained by taking the shear strength measured at zero suction as a reference datum. Figure 4.8 also shows that the variation of the $\emptyset^b$ angle with suction for AMU-HSC together with Bole and CMC area soils of Gebre (2010) and Zhan and Ng (2006) China soil samples.

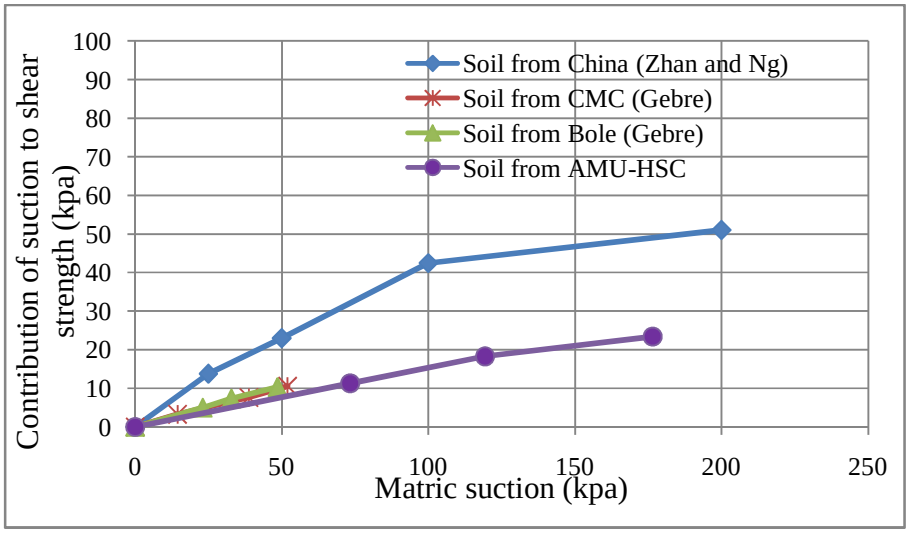

Figure 4-7 Contribution of suction to shear strength for AMU-HSC site together with Bole and CMC area soils of Gebre (2010) and China soils of Zhan and Ng (2006).

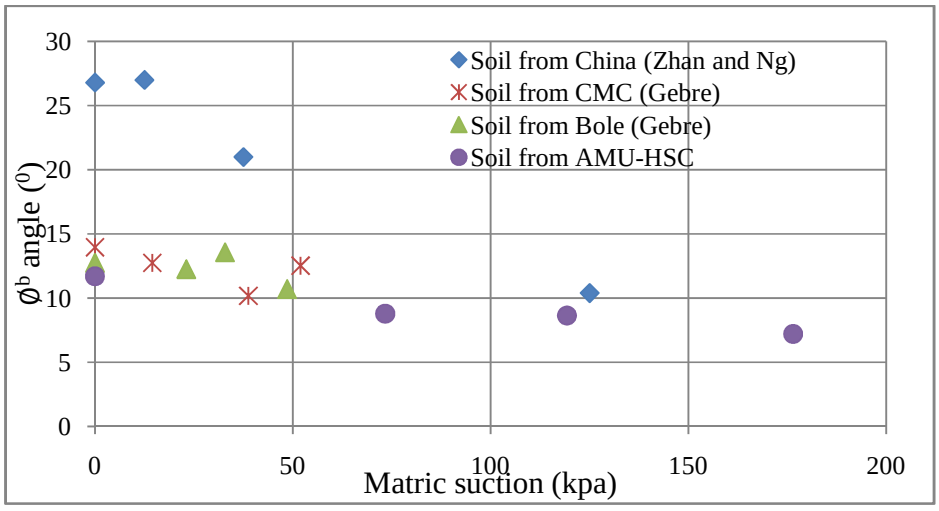

Figure 4-8 Variations of $\emptyset^b$ angles with matric suction for AMU-HSC together with Bole and CMC area soils of Gebre (2010) and China soils of Zhan and Ng (2006).

5. CONCLUSION AND RECOMMENDATION

5.1. **Conclusion**

The assessment on the existing swelling pressure predictive equations suggested by various authors reflected the need for developing specific equation for specific area. All the formulated models in this study predict the swelling pressure with various degrees of accuracy. Testing the validity of the new models provides reasonable results for equation 4.1 and 4.2.

Based on the results obtained from the consolidated undrained triaxial tests performed on expansive soils of AMU-HSC site for an unsaturated soil, it can be concluded that, when matric suction of the soil increases from 0kPa to 200kPa, the deviator stress of the soil increases from 107.61kPa to 174.35kPa for the effective consolidation pressure of 200 kPa. The shape of the stress-strain curve is kept unaltered for the raise in matric suction. Furthermore, as the matric suction of the soil increases, the shear strength of the soil increases nonlinearly for the applied matric suction ranges (i.e., 100kPa to 200kPa). However, the rates of increase in the apparent shear strength due to increase in matric suction, as expressed by the angle $\varnothing^{b}$ shows to decrease.

5.2. **Recommendation**

Although it is not expected to have an accurate swelling pressure result from empirical equation, an improved model can be fitted by increasing the database from tests done on a number of undisturbed samples during driest season. For preliminary estimation of the swelling characteristics of the study area, the formulated equations can be utilized.

Further detail investigation on the unsaturated state can be carried out by taking more number of samples and conducting the test on matric suctions out of the limit used (i.e., lower than 100kPa and higher than 200kPa) in order to see the effect. The nonlinearity of the shear stress versus matric suction becomes more noticeable when soils are being tested over a wider range of matric suctions.

List of References

Abed, A. (2008). *Numerical Modelling of Expansive Soil Behaviour*. Ph.D. Dissertation, Institut für Geotechnik, Universität Stuttgart, Germany.

Alla P. (2009). *Dynamic behavior of unsaturated soils***.** Msc. Thesis, Graduate Faculty of the Louisiana State University, U.S.A.

Al-Rawas, A.A. and Goosen, M.F. (2006). *Expansive soils: Recent advances in characterization and treatment.* Taylor & Francis Group, London, UK.

ASTM.(2004). *Standard Test Method for soil and rock*. Annual Book of ASTM Standards, Philadelphia, U.S.A.

Belachew, A (2000). *Dry-spell analysis for studying the sustainability of rain-fed agriculture in Ethiopia : the case of the Arba Minch area.* 8th Nile 2002 Conference, Addis Ababa, Ethiopia.

Blight, G. E. (1997). *Mechanics of Residual Soils*. A.A Balkema, Rotterdam, Netherlands.

British Standards Institution,(1990). *British standard methods of test for soils for civil engineering purposes*. British Standards Institution, London.

Budhu, M. (2007). *Soil Mechanics and Foundations*. 2nd ed., John Wiley & Sons Inc., New York.

Chakraborty, S. (2009). *Numerical Modeling for Long Term Performance of Soil-Bentonite Cut-Off Walls in Unsaturated Soil Zone*. Msc. Thesis, Graduate Faculty of the Louisiana State University, U.S.A.

Chen, F.H.(1988). *Foundation on Expansive Soils*. Elsevier scientific publishing company.

Craig, R.F.(2004). *Craig's Soil Mechanics*. 7th ed., Spon Press, London and New York.

CSA. (2007). *The 2007 Population and Housing Census of Ethiopia: Statistical Report for Southern Nations, Nationalities and Peoples' Region; Part I: Population Size and Characteristics.* http://www.csa.gov.et. 4/26/2011.

Das, B. M. (2002). *Principles of Geotechnical Engineering*. 5th ed., Thomson Learning, U.S.A.

Field, A. (2005). *Discovering Statistics using SPSS.* 2nd ed., SAGE publications, London.

Förch, G. (2009). *CICD Series Vol.3: Summary of Master Theses from Arba Minch University, Ethiopia*. Printing Office, Universität Siegen, Germany.

Fredlund, D.G. and Rahardjo, H.(1993). *Soil Mechanics for Unsaturated Soils*. John Wiley & Sons Inc. New York.

Gebre, H. (2010). *Unsaturated Shear Strength Characteristics and Stress Strain Behaviour Of Expansive Soils of Addis Ababa*. Msc. Thesis, Addis Ababa University, Addis Ababa, Ethiopia.

Gebrehiwot, T. (2003). *Ameliorated Design and Construction Techniques of Pavements on Expansive Soils.* Msc. Thesis, Addis Ababa University, Addis Ababa, Ethiopia.

İkizler, S. B., Aytekin, M., and Nas, E. (2007). *The Variation of Swelling Characteristics with EPS Geofoam in Expansive Soils.* 18th European Young Geotechnical Engineers' Conference, Portonovo, Ancona, Italy.

Kerry Rowe, R. (2001). *Geotechnical and Geoenvironmental Engineering Hand Book*. Kulwer Academic Publishers, USA, 2001.

Komornik, J. and David, A.(1969). *Prediction of swelling potential for compacted clays*. Journal of the Soil Mechanics and Foundation Engineering Division, ASCE, Vol. 95, No. 1, 209–225, 1969.

Legesse, M. (2004). *Investigating Index Property of Expansive Soil of Ethiopia*. Msc Thesis, Addis Ababa University, Addis Ababa, Ethiopia.

Lu, N. and Likos, W.J.(2004). *Unsaturated soil Mechanics*. John Wiley & Sons Inc. New Jersey.

Murray, H.H.(2007). *Applied Clay Mineralogy:* Occurrences, Processing and Application of Kaoines, Bentonites, Palygorskite-Sepiolite, and Common Clays. Elsevier scientific publishing company.

Nayak, N.V. and Chiristensen, R.W.(1974). *Swelling characteristics of compacted expansive soils.* Clays and Clay Minerals, Vol. 19, No. 4, 251–261.

Nelson, J.D. and Miller, D.J. (1992). *Expansive Soils: Problems and Practice in Foundation and Pavement Engineering*. New York: Wiley Interscience.

Nigussie D. (2007). *Indepth Investigation of Relationship between Index Property and Swelling Characteristics of Expansive soil in Bahir Dar*. Msc. Thesis, Addis Ababa University, Addis Ababa, Ethiopia.

Ng, C.W.W and Menizies, B. (2007). *Advanced unsaturated soil Mechanics and Engineering.* Taylor &Francis Group, London and New York.

Sabtan, A. A., (2005). Geotechnical properties of expansive clay shale in Tabuk, Saudi Arabia. Journal of Asian Earth Sciences 25, 747 -757, Elsevier scientific publishing company.

Sime, A., (2006). *Further Investigation of Road Failures Constructed on Expansive Soils of Central Ethiopia: Addis Ababa –Jimma Road as a case Study.* Msc. Thesis, Addis Ababa University, Addis Ababa, Ethiopia.

Stephen G. F., Donald A.C., and Paul F.W.(2005). *The shrink Swell Test.* Geotechnical Testing Journal, Vol. 28, No.1.

Teferra, A. (2009). *Principles of Foundation Engineering*. 2nd ed. Addis Ababa University Press, Addis Ababa.

Teferra, A. And Leikun, M. (1999). *Soil Mechanics*. Addis Ababa University press. Addis Ababa.

Teklu, D. (2003). *Examining the swelling pressure of Addis Ababa Expansive soil*. Msc Thesis, Addis Ababa University Technology Faculty, Addis Ababa, Ethiopia.

Terzaghi, K.(1943). *Theoretical soil mechanics*. Wiley Publications, New York.

Tilahun, D. (2004). *Influence of Drainage Condition on Shear Strength Parameters of Expansive soils.* Msc Thesis, Addis Ababa University Technology Faculty, Addis Ababa, Ethiopia.

Ulusay R. (2002). *A simple test and predictive models for assessing swell potential of Ankara (Turkey) Clay*. Elsevier scientific publishing company.

Vijayavergiya, V.N. and Ghazzaly, O.I. (1973). *Prediction of swelling potential for natural clays.* Proceedings of 3rd International Conference on Expansive Soils, Haifa, Israel, Vol. 1, 227–236.

W/Medhin G., (2010). *A Study on Shear Strength Characteristics of Addis Ababa Red Clay Soil for Unsaturated Case.* Msc Thesis, Addis Ababa University, Addis Ababa, Ethiopia.

Zewdie, A. (2004). *Investigation into shear strength characteristics of Expansive soil of Ethiopia*. Msc Thesis, Addis Ababa University, Addis Ababa, Ethiopia.

Zhan, T. L. T. and Ng, C. W. W. (2006). *Shear Strength characteristics of an unsaturated expansive clay.* Canadian Geotechnical Journal, Vol.43, 7, pp. 751-763.

Appendix

Appendix-A

Table A-1 Data sheet for Liquid and Plastic Limit test for AMU – HSC site

	Liquid Limit				Plastic Limit	
Trial No	1	2	3	4	1	2
Number of blows	18	21	27	33	----	----
Can Number	47	D16	DEF	D8	33	A17
Mass of can, g	15.39	15.56	15.62	15.5	14.06	15.79
Mass of can + Wet soil, g	35.92	36.17	38.75	35.33	16.88	18.87
Mass of container + Dry soil, g	24.61	24.9	26.119	24.62	15.99	17.89
Mass of water, g	11.31	11.27	12.631	10.71	0.89	0.98
Mass of dry soil, g	9.22	9.34	10.499	9.12	1.93	2.1
Moisture content, %	122.67	120.66	120.31	117.43	46.11	46.67

Liquid limit,% = 119.93 Plastic limit,% = 46.39 PI,% = 73.54

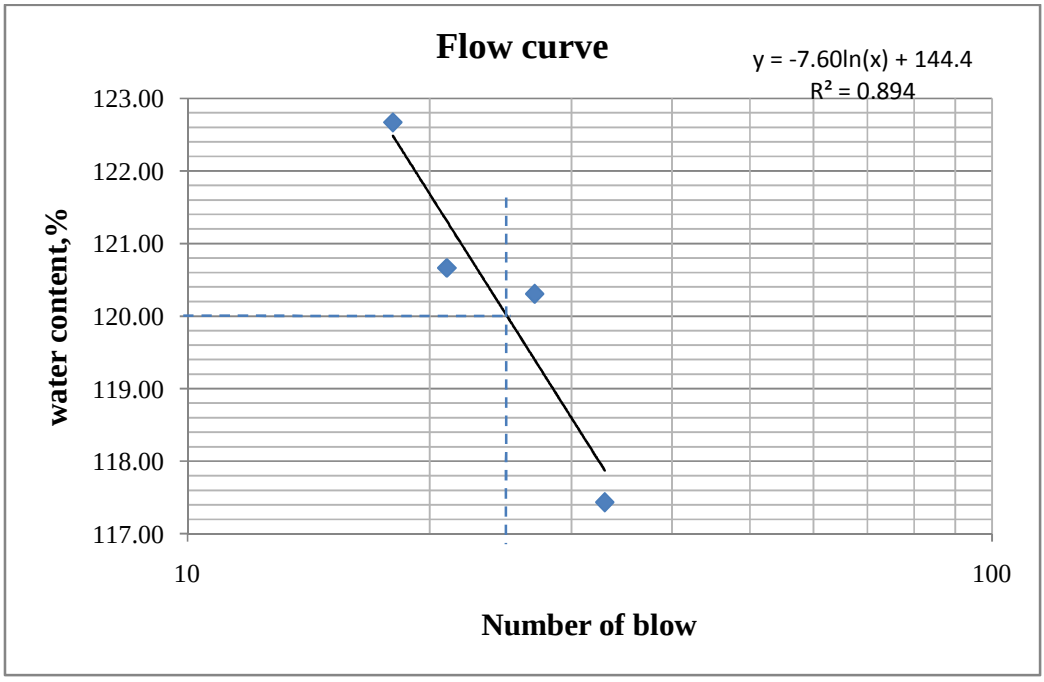

Figure A-1 Flow curve for soil from AMU – HSC site

Table A-2 Data sheet for Volumetric Shrinkage Limit test for AMU – HSC site

Trial	1	2
Shrinkage dish no.	E	B
Mass of wet soil + coated shrinkage dish (m_3), g	93.29	91.43
Mass of dry soil + coated shrinkage dish (m_4), g	58.97	57.43
Mass of coated shrinkage dish (m_2), g	24.70	24.30
Mass of wet soil ($m_1 = m_3 - m_2$), g	68.60	67.13
Mass of dry soil ($m_d = m_4 - m_2$), g	34.27	33.13
Mass of water, (m_1-m_4), g	34.32	34.00
Moisture content, $w_o = (m_1-m_4)/m_d$, %	100.15	102.63
Mass of Mercury in shrinkage dish (full) + mercury dish, g	662.00	643.00
Mass of dissplaced Mercury + Mercury dish, g	428.00	433.00
Mass of Mercury dish, g	24.70	24.30
Volume of Mercury in shrinkage dish (Vol. of wet soil) V_o, cc	47.10	45.73
Vol. of Mercury displaced by dry soil (Vol. of oven dried soil) V_f, cc	17.29	15.52
Shrinkage limit, $w_s = w_o - (V_o - V_f)/m_d*1*100$, %	13.17	11.45
Average Shrinkage Limit, %	12.31	

Table A-3 Data sheet for wet sieve analysis test for AMU – HSC site

Wet Sieve Analysis Total mass of sample, g 1088

Sieve No	Sieve Opening (mm)	Mass of Sieve (g)	Mass of sieve + Retained soil (g)	Mass of Retained soil (g)	Percentage Retained (%)	Cum. Percentage Retained (%)	Perc. Passing (%)
3"	75.0	424.0	424.0	0.0	0.0	0.0	100.0
2.5"	50.0	442.0	442.0	0.0	0.0	0.0	100.0
2"	37.5	434.0	434.0	0.0	0.0	0.0	100.0
1.5"	25.0	469.0	469.0	0.0	0.0	0.0	100.0
1"	19.0	455.0	455.0	0.0	0.0	0.0	100.0
3/4"	12.5	443.0	443.0	0.0	0.0	0.0	100.0
1/2"	9.5	442.0	442.0	0.0	0.0	0.0	100.0
3/8"	4.75	446.0	446.0	0.0	0.0	0.0	100.0
No 4	2.36	429.0	438.0	9.0	0.8	0.8	99.2
No 10	2	377.0	393.0	16.0	1.5	2.3	97.7
No 40	0.425	293.0	315.0	22.0	2.0	4.3	95.7
No 200	0.075	272.0	282.0	10.0	0.9	5.2	94.8
pan	----	255.0	1286.0	1031.0	94.8	94.8	-------

Table A-4 Data sheet for Hydrometer analysis test for AMU – HSC site

Hydrometer No. 151H			Lab Temperature: 19.2 °c		Specific Gravity = 2.72			
Elapsed Time (min)	Actual Hydrometer Reading	Composite Correction	Corrected Hydrometer Reading	Effective Depth (cm)	Coefficient K	Grain Size (mm)	Perc. Finer (%)	Perc. Finer Combined (%)
0.75	1.0320	-0.00276	1.0292	7.84	0.01345	0.0435	92.48	87.63
1	1.0310	-0.00276	1.0282	8.10	0.01345	0.0383	89.32	84.64
2	1.0305	-0.00276	1.0277	8.23	0.01345	0.0273	87.74	83.14
4	1.0295	-0.00276	1.0267	8.50	0.01345	0.0196	84.57	80.14
8	1.0280	-0.00276	1.0252	8.89	0.01345	0.0142	79.83	75.65
15	1.0270	-0.00276	1.0242	9.16	0.01345	0.0105	76.67	72.65
30	1.0255	-0.00276	1.0227	9.55	0.01345	0.0076	71.92	68.15
60	1.0240	-0.00276	1.0212	9.95	0.01345	0.0055	67.18	63.66
120	1.0225	-0.00276	1.0197	10.35	0.01345	0.0039	62.43	59.16
240	1.0215	-0.00276	1.0187	10.61	0.01345	0.0028	59.27	56.17
480	1.0210	-0.00276	1.0182	10.75	0.01345	0.0020	57.69	54.67
1440	1.0190	-0.00276	1.0162	11.27	0.01345	0.0012	51.36	48.67

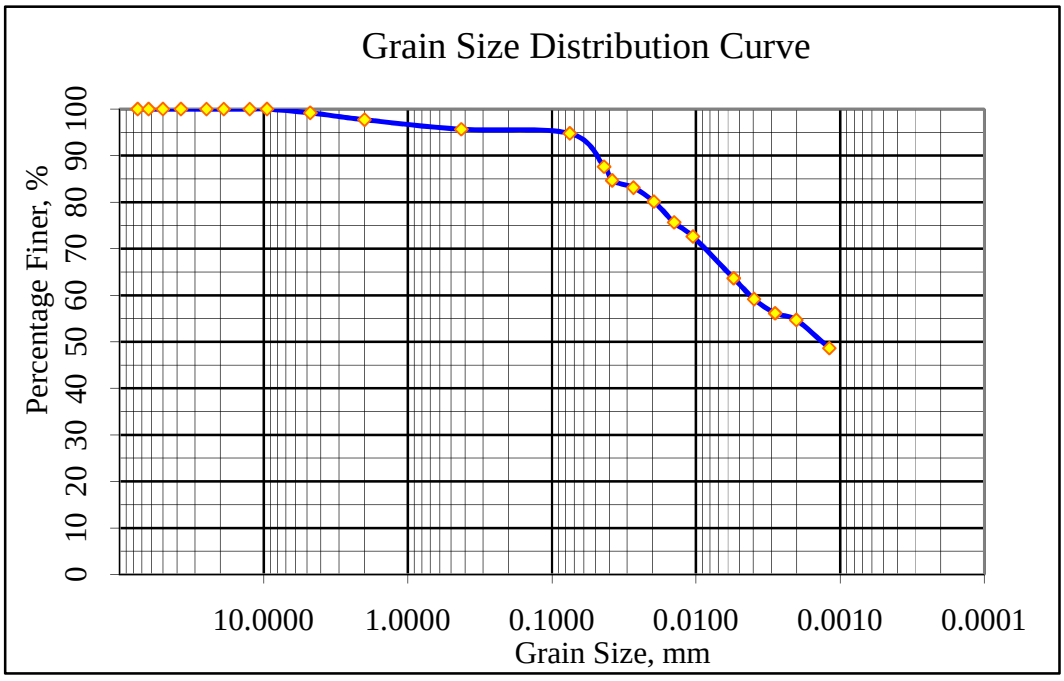

Figure A-2 Grain size curve for AMU–HSC site

For the consolidation test, the initial void ratio is back calculated from the final void ratio as follows:

1. At the end of the test, the specimen is removed from the oedometer and the water content is measured. Since the specimen is fully saturated, the void ratio of the specimen at the end of test can be found from: $e_f = \omega G_s$
2. The initial void ratio can be related to the final as: $e_f = e_o - \Delta e$
3. The two unknowns above, e_o and Δe, can be solved from the total change in height between the initial and the final condition, or Δz_f to give:

$$e_o = \frac{e_f + \frac{\Delta z_f}{H_o}}{1 - \frac{\Delta z_f}{H_o}}$$

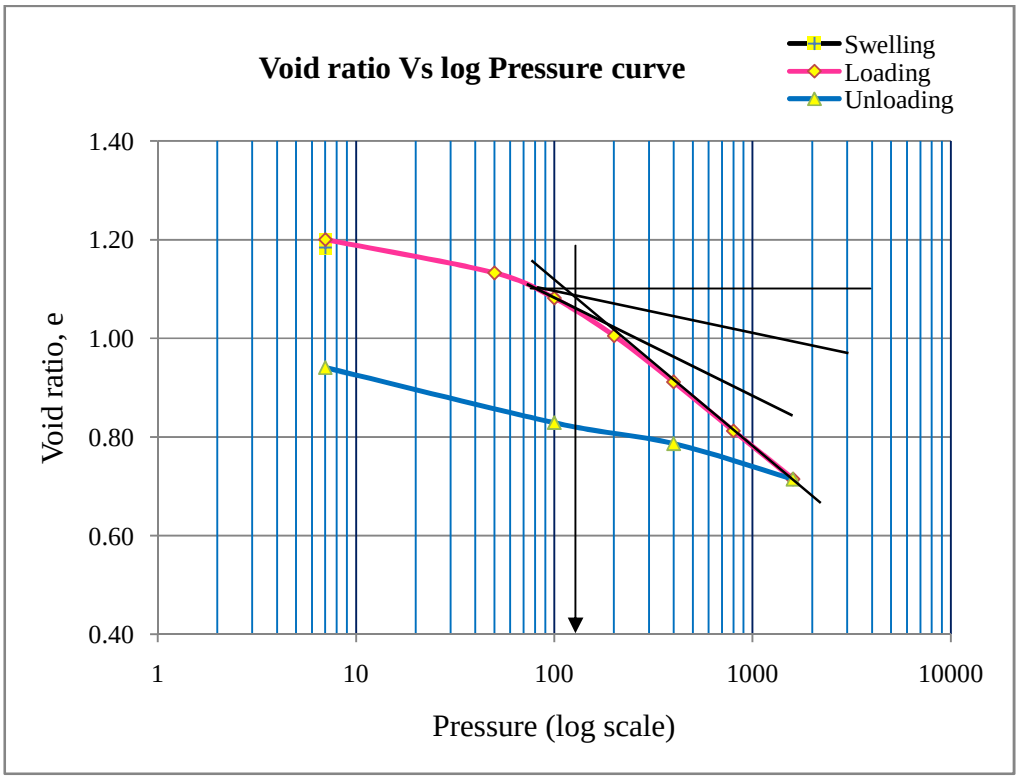

Figure A-3 Void ratio Vs log Pressure curve for preconsolidation pressure of AMU–HSC site

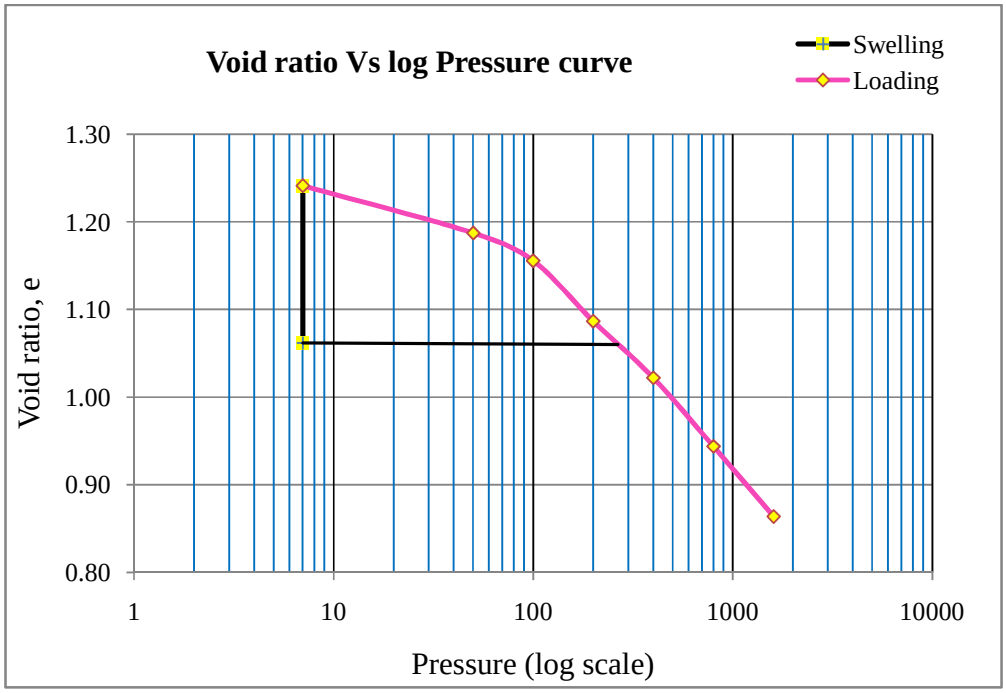

Figure A-4 Void ratio Vs log Pressure curve for swelling pressure of AMU–HSC site

Table A-5 Data sheet for Swelling pressure test for AMU-HSC site

			$\omega_f = 31.75\%; G_s = 2.72$	
Applied pressure P (kPa)	Final Dial Reading (mm)	Change in Specimen Height (mm)	Final Specimen Height (mm)	Void Ratio, e
Loading				
7	6.201	0.00	20.00	1.06
7	4.459	-1.74	21.74	1.24
50	4.984	-1.22	21.22	1.19
100	5.290	-0.91	20.91	1.16
200	5.961	-0.24	20.24	1.09
400	6.586	0.39	19.62	1.02
800	7.345	1.14	18.86	0.94
1600	8.123	1.92	18.08	0.86

Table A-6 Data sheet for Liquid and Plastic Limit test for Yetnebersh site

	Liquid Limit				Plastic Limit	
Trial No	1	2	3	4	1	2
Number of blows	19	24	30	34	-----	-----
Can Number	9	61	72	101	A76	A1
Mass of can, g	15.68	15.52	15.69	15.55	15.56	11.5
Mass of can + Wet soil, g	42.71	39.17	50.27	40.96	19.57	15.81
Mass of can + Dry soil, g	28.633	26.93	32.45	27.89	18.25	14.39
Mass of water, g	14.077	12.24	17.82	13.07	1.32	1.42
Mass of dry soil, g	12.953	11.41	16.76	12.34	2.69	2.89
Moisture content, %	108.68	107.27	106.32	105.92	49.07	49.13

Liquid limit,% = 107.25 Plastic limit,% = 49.10 PI,% = 58.15

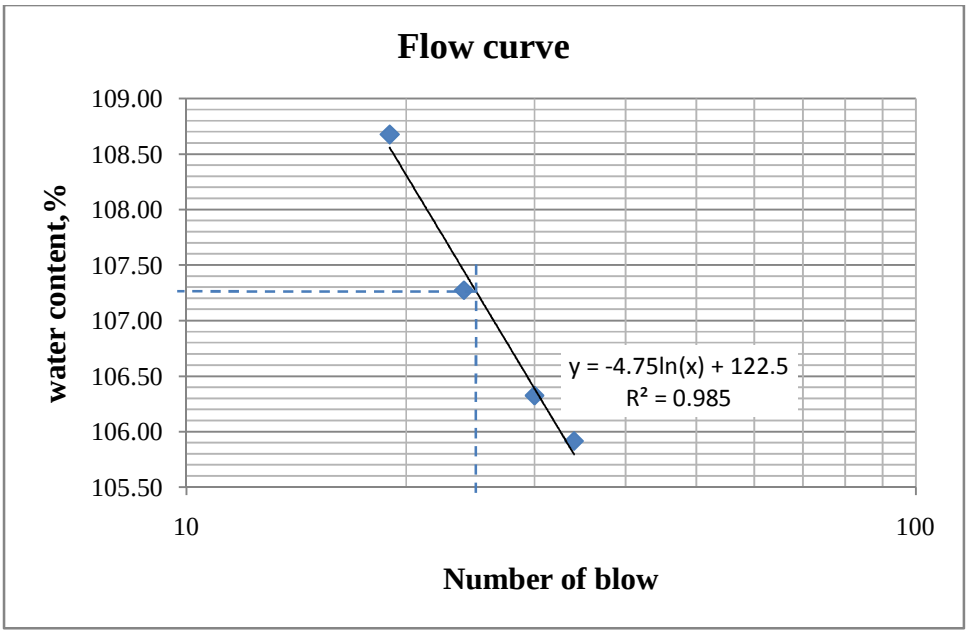

Figure A-5 Flow curve for soil from Yetnebersh site

Table A-7 Data sheet for Volumetric Shrinkage Limit test for Yetnebersh site

Trial	1	2
Shrinkage dish no.	C-5	B
Mass of wet soil + coated shrinkage dish (m_3), g	41.97	94.34
Mass of dry soil + coated shrinkage dish (m_4), g	30.68	60.53
Mass of coated shrinkage dish (m_2), g	19.60	24.64
Mass of wet soil ($m_1 = m_3 - m_2$), g	22.37	69.70
Mass of dry soil ($m_d = m_4 - m_2$), g	11.08	35.89
Mass of water, (m_1-m_4), g	11.30	33.81
Moisture content, $w_o = (m_1-m_4)/m_d$, %	101.96	94.20
Mass of Mercury in shrinkage dish (full) + mercury dish, g	227.00	659.00
Mass of dissplaced Mercury + Mercury dish, g	154.00	428.00
Mass of Mercury dish, g	19.60	24.64
Volume of Mercury in shrinkage dish (Vol. of wet soil) V_o, cc	15.33	46.89
Vol. of Mercury displaced by dry soil (Vol. of oven dried soil) V_f, cc	5.40	17.07
Shrinkage limit, $w_s = w_o - (V_o - V_f)/m_d*1*100$, %	12.29	11.14
Average Shrinkage Limit, %	11.71	

Table A-8 Data sheet for Wet sieve analysis test for Yetnebersh site

Wet Sieve Analysis — Total mass of sample, g 2040

Sieve No	Sieve Opening (mm)	Mass of Sieve (g)	Mass of sieve + Retained soil (g)	Mass of Retained soil (g)	Percentage Retained (%)	Cum. Percentage Retained (%)	Perc. Passing (%)
3"	75.0	424.0	424.0	0.0	0.0	0.0	100.0
2.5"	50.0	442.0	442.0	0.0	0.0	0.0	100.0
2"	37.5	434.0	434.0	0.0	0.0	0.0	100.0
1.5"	25.0	469.0	469.0	0.0	0.0	0.0	100.0
1"	19.0	455.0	455.0	0.0	0.0	0.0	100.0
3/4"	12.5	443.0	443.0	0.0	0.0	0.0	100.0
1/2"	9.5	442.0	442.0	0.0	0.0	0.0	100.0
3.8"	4.75	446.0	446.0	0.0	0.0	0.0	100.0
No 4	2.36	429.0	448.0	19.0	0.9	0.9	99.1
No 10	2	377.0	399.0	22.0	1.1	2.0	98.0
No 40	0.425	293.0	310.0	17.0	0.8	2.8	97.2
No 200	0.075	272.0	303.0	31.0	1.5	4.4	95.6
pan	----	255.0	2206.0	1951.0	95.6	95.6	-------

Table A-9 Data sheet for Hydrometer analysis test for Yetnebersh site

Hydrometer No. 151H			Lab Temperature: 18 °c		Specific Gravity = 2.69			
Elapsed Time (min)	Actual Hydrometer Reading	Composite Correction	Corrected Hydrometer Reading	Effective Depth (cm)	Coefficient K	Grain Size (mm)	Perc. Finer (%)	Perc. Finer Combined (%)
0.75	1.0325	-0.0031	1.0294	7.70	0.013822	0.0443	93.59	89.51
1	1.0320	-0.0031	1.0289	7.84	0.013822	0.0387	92.00	87.99
2	1.0315	-0.0031	1.0284	7.97	0.013822	0.0276	90.41	86.47
4	1.0310	-0.0031	1.0279	8.10	0.013822	0.0197	88.82	84.94
8	1.0305	-0.0031	1.0274	8.23	0.013822	0.0140	87.23	83.42
15	1.0295	-0.0031	1.0264	8.50	0.013822	0.0104	84.04	80.38
30	1.0290	-0.0031	1.0259	8.63	0.013822	0.0074	82.45	78.85
60	1.0275	-0.0031	1.0244	9.03	0.013822	0.0054	77.68	74.29
120	1.0260	-0.0031	1.0229	9.42	0.013822	0.0039	72.90	69.72
240	1.0250	-0.0031	1.0219	9.69	0.013822	0.0028	69.72	66.68
480	1.0240	-0.0031	1.0209	9.95	0.013822	0.0020	66.53	63.63
1440	1.0235	-0.0031	1.0204	10.08	0.013822	0.0012	64.94	62.11

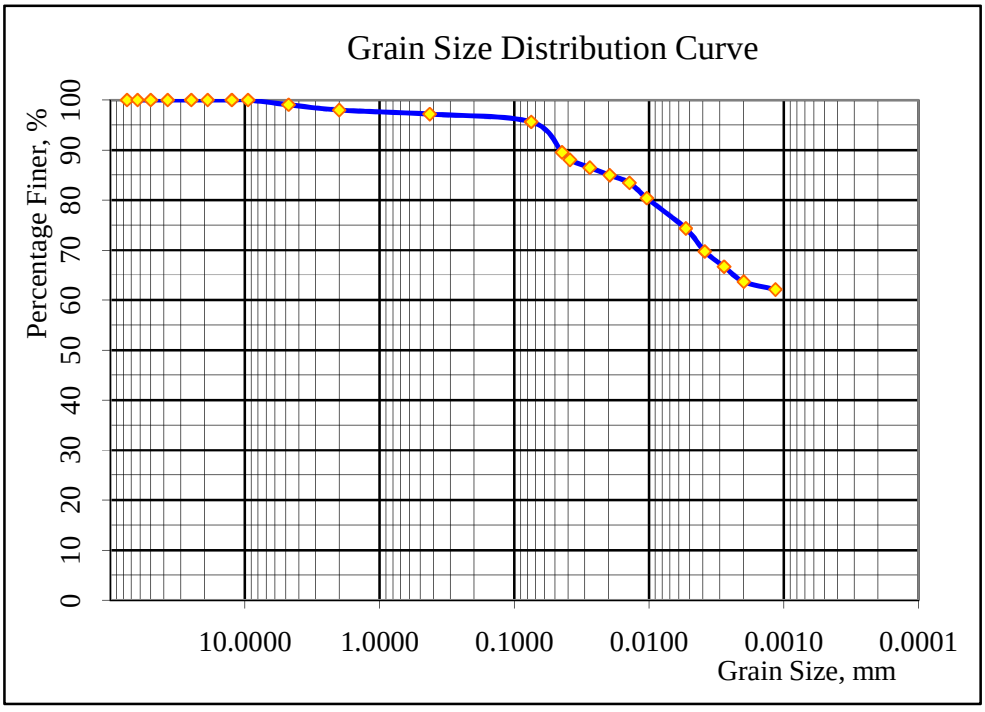

Figure A-6 Grain size curve for Yetnebersh site

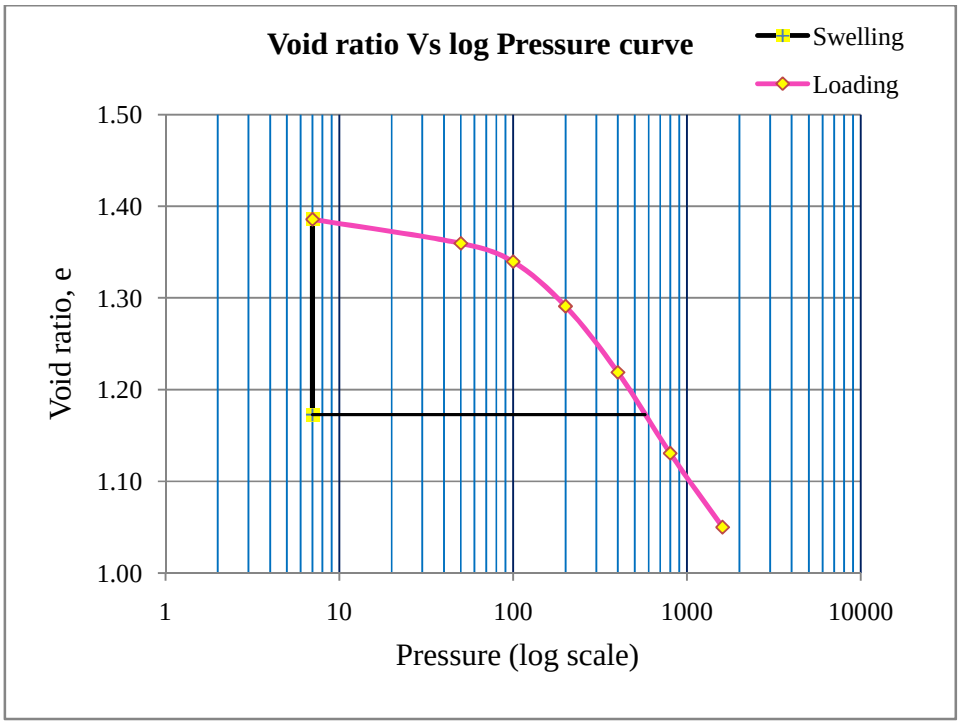

Figure A-7 Void ratio Vs log Pressure curve for swelling pressure of Yetnebersh site

Table A-10 Data sheet for Swelling pressure test for Yetnebersh site

			$\omega_f = 39.03\%; G_s = 2.69$	
Applied pressure P (kPa)	Final Dial Reading (mm)	Change in Specimen Height (mm)	Final Specimen Height (mm)	Void Ratio, e
Loading				
7	4.300	0.00	20.00	1.17
7	2.340	-1.96	21.96	1.39
50	2.579	-1.72	21.72	1.36
100	2.764	-1.54	21.54	1.34
200	3.212	-1.09	21.09	1.29
400	3.874	-0.43	20.43	1.22
800	4.690	0.39	19.61	1.13
1600	5.430	1.13	18.87	1.05

Table A-11 Parameters used to draw the Mohr circles for saturated soils (results obtained from the consolidated undrained test)

Site	**Sample No**	σ_3	Excess pore water Δu_w	$(\sigma_1 - \sigma_3)$	σ_1	$\sigma'_1 = \sigma_1 - \Delta u_w$	$\sigma'_3 = \sigma_3 - \Delta u_w$
AMU-HSC	S-1	200	108.76	107.61	307.61	198.85	91.24
	S-2	250	115.83	133.23	383.23	267.40	134.17
	S-3	300	127.95	149.19	449.19	321.24	172.05

Table A-12 Parameters used to draw the Mohr circles for unsaturated soils (results obtained from the consolidated undrained test)

Site	**Sample No**	σ_3	h_m	Excess pore air Δu_a	Excess pore water Δu_w	$h_{m(at\ failure)}$	$(\sigma_1 - \sigma_3)$	σ_1	$\sigma'_1 = \sigma_1 - \Delta u_a$	$\sigma'_3 = \sigma_3 - \Delta u_a$
AMU-HSC	S-4	200	100	106.47	133.13	73.34	138.24	338.24	231.77	93.53
	S-5	200	150	98.92	129.64	119.28	157.22	357.22	258.30	101.08
	S-6	200	200	89.76	113.30	176.46	174.35	374.35	284.59	110.24

Appendix-B

(a) (b)

Figure B-1 (a) Sampling undisturbed soil in the field; (b) carefully wrapped sample ready for test specimen extraction.

Figure B-2 Extruding undisturbed soil specimen from the sampling tube

Figure B-3 Conventional triaxial machine used for testing saturated samples

(a) (b)

Figure B-4 Soil sample mounted on (a) Conventional triaxial equipment, (b) Modified triaxial machine.

Figure B-5 Typical soil sample after shearing